



*Supplement of*

## **Aerosol water parameterization: a single parameter framework**

**S. Metzger et al.**

*Correspondence to:* S. Metzger (s.metzger@cyi.ac.cy, swen.metzger@mpic.de)

The copyright of individual parts of the supplement might differ from the CC-BY 3.0 licence.

# 1 S1 Examples – Semi-volatile compounds

2 The following three sub-sections provide detailed examples for semi-volatile compounds,  
 3 described in Sec. 2.4 (main text). The analytical solution is part of our new single  
 4 parameter gas-liquid-solid partitioning framework and applied in Sec. 3 to mixed aerosol  
 5 salt solutions through EQSAM4clim (see Appendix B and Sec. S2).

## 6 S1.1 Pure $\text{NH}_4\text{NO}_3$ –gas-solid equilibrium ( $\text{RH} < \text{RHD}$ )

7 Gas-solid equilibrium of pure ammonium nitrate;  $\text{NH}_4\text{NO}_3$  (index  $_{AN}$ ) with  $\text{RH} = 50\%$   
 8 and below the  $\text{RHD}_{AN} = 61.83\%$  (Table 1), as illustrated in Fig. 3. The partial pres-  
 9 sure product of gaseous ammonia,  $\text{NH}_3(\text{g})$ , and nitric acid,  $\text{HNO}_3(\text{g})$  must equal or exceed  
 10  $K_p(T)$  to allow the formation of solid ammonium nitrate,  $\text{NH}_4\text{NO}_3(\text{s})$ . This is described  
 11 by (R-1) and the system can be solved with Eqs. (6–12). Note that in this case, only the  
 12 gas phase concentrations are required to solve (R-1), since the concentrations of solids  
 13 are treated as unity. Here, all concentrations denoted by  $[\ ]$  are given in  $[\mu\text{mol}/\text{m}^3(\text{air})]$ ;  
 14 the EQSAM4clim computations (see Sec. S2) are performed in  $[\text{mol}/\text{m}^3(\text{air})]$ . For com-  
 15 parison with SP2006, we use ppbv. Units, e.g., in  $[\mu\text{mol}/\text{m}^3(\text{air})]$  can be converted to  
 16 ppbv by multiplication with the molar volume  $24.465 [\text{L}/\text{mol}]$ , and from  $[\mu\text{g}/\text{m}^3(\text{air})]$  by  
 17 additional division with the compounds molar mass,  $M_s$ .

18 At  $T_o = 298.15 \text{ K}$ ,  $P_o = 1 \text{ atm}$  and  $\text{RH} = 50\%$  (i.e.,  $\text{RH} < \text{RHD}_{AN}$ ), with  $M_s$  in  
 19 units of  $[\text{g}/\text{mol}]$  (and  $1 \text{ ppbv} = 1 \text{ nano Liter gas per 1 Liter air} = 1 \text{ micro Liter(gas) per}$   
 20  $\text{m}^3(\text{air})$ ), the unit conversion to  $[\text{ppbv}]$  from concentrations in  $[\mu\text{g}(\text{gas})/\text{m}^3(\text{air})]$  yields,  
 21 e.g., for  $\text{NH}_3(\text{g})=17.04$  and  $\text{HNO}_3(\text{g})=63.02$  (see example on p474 of SP2006):

- 22 •  $\text{NH}_3(\text{g}) : 17.04 [\mu\text{g}(\text{gas})/\text{m}^3(\text{air})] / 17.04 [\text{g}/\text{mol}] \cdot 24.465 [\text{L}/\text{mol}] = 24.465 [\text{ppbv}]$
- 23 •  $\text{HNO}_3(\text{g}) : 63.02 [\mu\text{g}(\text{gas})/\text{m}^3(\text{air})] / 63.02 [\text{g}/\text{mol}] \cdot 24.465 [\text{L}/\text{mol}] = 24.465 [\text{ppbv}]$

24 The partial pressure product is  $24.465^2 \approx 600 [\text{ppbv}^2]$  and at this  $T$  well above the  
 25 equilibrium value of  $K_{p,AN}(T) = 57.5 [\text{ppbv}^2]$  (Table 4; Fig. 1), but lower than the value  
 26 of  $655 [\text{ppbv}^2]$  given in SP2006, which corresponds to  $T = 308 [\text{K}]$ .

27 Following SP2006 for this dry case, the amount  $x [\text{ppbv}]$  of the gaseous concentration  
 28  $C_i [\text{ppbv}]$ , which could form a solid, can be directly computed by solving the equation:

$$\prod_{i=1}^n (C_i - x) = K_p(T) \quad (\text{S1})$$

29 For ammonium nitrate, (R-1) yields a quadratic equation (with  $a \cdot x^2 - 2 \cdot b \cdot x + c = 0$ )  
 30  $(24.5 - x)(24.5 - x) = 57.5 [\text{ppbv}^2]$ , i.e.,  $x^2 - 49x + 543 = 0$ . And, upon solving (with  
 31  $x_{1,2} = 0.5 \cdot (-b \pm \sqrt{(b^2 - 4 \cdot a \cdot c)}) / a$ ), i.e.,:  $x_1 = 0.5 \cdot (49 - \sqrt{(2401 - 4 \cdot 543)}) \approx 16.9 [\text{ppbv}]$ .  
 32 Note that the second solution ( $x_2 \approx 32.1$ ) is to be discarded, since its value is larger than  
 33 the actual  $C_i$  concentrations. Thus, an equal amount of  $16.9 [\text{ppbv}]$  of each  $\text{NH}_3(\text{g})$  and  
 34  $\text{HNO}_3(\text{g})$  and solid  $\text{NH}_4\text{NO}_3(\text{s})$  would be in equilibrium at this temperature and RH.  
 35 In terms of mass loadings, this corresponds to  $11.8$  and  $43.5$  and  $55.2 [\mu\text{g}/\text{m}^3(\text{air})]$ ,  
 36 respectively. The mass loadings of the corresponding residual (free) acids are:  $\text{NH}_3(\text{g}) =$   
 37  $(24.5 - 16.9) / 24.5 \cdot 17 = 5.3$  and  $\text{HNO}_3(\text{g}) = (24.5 - 16.9) / 24.5 \cdot 63 = 19.5 [\mu\text{g}/\text{m}^3(\text{air})]$ ,  
 38 respectively. This case is illustrated in Fig. 3 (see upper panels); Sec. 2.4.1 and 2.5.

## 39 S1.2 Pure $\text{NH}_4\text{NO}_3$ -gas-liquid equilibrium ( $\text{RH} \geq \text{RHD}$ )

40 Same as the first example, but with  $\text{RH} = 80\%$  and above the  $\text{RHD}_{\text{AN}}$ . In line with  
 41 the dry case (Sec. 2.4.1 and S1.1), the amount  $x$  [ppbv] of the gaseous concentration  
 42  $C_i$  [ppbv], which could form aqueous ammonium nitrate, can be directly computed with  
 43 Eqs. (6–12), if Eqs. (2–3) are used to solve  $K_p(T, \text{RH})$  (see Sec. 2.4.2). Then, (R-1) can  
 44 be analogously solved by using Eq. (S1) of the above dry case (Sec. S1.1):

$$\prod_{i=1}^n (C_i - x) = K_p(T, \text{RH}) \quad (\text{S2})$$

45 For instance, considering the gas-aqueous phase equilibrium of ammonium nitrate at  
 46  $\text{RH} = 80\%$ , by assuming that the water activity  $a_w$  equals  $\text{RH}/100$ , we can obtain a  
 47 value of 10 [ $\text{mol}_{\text{AN}}/\text{kg}(\text{H}_2\text{O})$ ] of the corresponding solute molality,  $\mu_{\text{AN}}(a_w = 0.8)$ , from  
 48 measurements, or from Eq. (A3) of Sec. A2; both are shown in Fig. A1 (in Sec. B). Using  
 49 Eq. (S2), with  $M_s = 0.08$  [ $\text{kg}/\text{mol}$ ] (of Table 1), we find for the solute mass fraction  
 50 (using Eq. A1) the corresponding value of:  $\chi_{\text{AN}}(a_w = 0.8) = (\frac{1}{0.08 \cdot 10} + 1)^{-1} = 0.44$ . And  
 51 from Eq. (3) we obtain,  $\text{COEF}_{\text{AN}}(\text{RH} = 80\%) = 2 \cdot 0.44^2 = 0.39$ , so that we can directly  
 52 obtain the required value for the T- and RH-dependent ammonium nitrate equilibrium  
 53 dissociation constant from Eq. (S2). At  $T = 298$  (using the value given in Table 4) we  
 54 accordingly find  $K_{p,\text{AN}}(T = 298, \text{RH} = 80\%) = 57.5 \cdot 0.39 \approx 22$  [ppbv<sup>2</sup>].

55 Mozurkewich (1993) gives a  $K_p^o(T_o)$  value of 42 [ppbv<sup>2</sup>], for which we would obtain at  
 56  $\text{RH} = 80\%$ ,  $41.9 \cdot 0.39 \approx 16$  [ppbv<sup>2</sup>] and accordingly  $\approx 12$  [ppbv<sup>2</sup>] for the value 29.9 [ppbv<sup>2</sup>],  
 57 which was originally given by Pilinis and Seinfeld (1987) (e.g., for use in the thermo-  
 58 dynamic model SEQUILIB). For EQSAM4clim, either  $K_p^o(T_o)$  value can be used. The  
 59 corresponding value of SP2006 (given in their example below Eq. (10.99)) is  $\approx 15$  [ppbv<sup>2</sup>].

60 Thus, knowing  $K_{p,\text{AN}}(T, \text{RH})$  one can directly solve the quadratic equation Eq. (S2)  
 61 for the aqueous phase analogously to Eq. (S1) for the dry case, without any iterations.  
 62 Using  $K_{p,\text{AN}}(T = 298, \text{RH} = 80\%) \approx 22$  [ppbv<sup>2</sup>] and the gas concentration for the solid  
 63 example given for Eq. (S1), we obtain for the equilibrium concentrations at  $\text{RH} = 80\%$ :  
 64  $(24.5 - x)(24.5 - x) = 57.5 \cdot 0.39 \approx 22$ , i.e.,  $x^2 - 49x + 578 = 0$ . And, upon solving the  
 65 quadratic equation  $x_1 = 0.5 \cdot (49 - \sqrt{(2401 - 4 \cdot 578)}) = 19.8$  [ppbv] (the second solution  
 66 has to be discarded, since its value is always larger than the actual  $C_i$  concentrations).  
 67 Using  $K_{p,\text{AN}}(T = 298, \text{RH} = 80\%) \approx 16$  [ppbv<sup>2</sup>] yields  $x = 20.5$  [ppbv], while using the ppb  
 68 values of the example of SP2006 gives  $(5 - x)(6 - x) = 15$ , i.e.,  $x^2 - 11x + 15 = 0$ , which  
 69 yields  $x_1 = 0.5 \cdot (11 - \sqrt{(121 - 4 \cdot 15)}) = 1.6$  [ppbv]. Thus, an equal amount 19.8 (20.5, 1.6)  
 70 [ppbv] of each  $\text{NH}_3(\text{g})$  and  $\text{HNO}_3(\text{g})$  and aqueous  $\text{NH}_4\text{NO}_3(\text{aq})$  would be in equilibrium at  
 71 this temperature and RH. The corresponding mass loadings of the residual (free) acids  
 72 are:  $(24.5 - 19.8)/24.5 \cdot 17 = 3.3$  and  $(4.7)/24.5 \cdot 63 = 12.1$  [ $\mu\text{g}/\text{m}^3(\text{air})$ ], respectively,  
 73 and those of the aqueous cation and anion are:  $\text{NH}_4^+(\text{aq}) = 19.8/24.5 \cdot 18 = 14.6$ , and  
 74  $\text{NO}_3^-(\text{aq}) = 19.8/24.5 \cdot 62 = 50.1$  [ $\mu\text{g}/\text{m}^3(\text{air})$ ]. The sum,  $14.6 + 50.1 = 64.7$  [ $\mu\text{g}/\text{m}^3(\text{air})$ ]  
 75 forms  $\text{NH}_4\text{NO}_3(\text{aq})$  and would be in equilibrium with  $\text{NH}_3(\text{g}) = 17.04$  and  $\text{HNO}_3(\text{g}) = 63.02$   
 76 [ $\mu\text{g}/\text{m}^3(\text{air})$ ] at  $T = 298.15$  [K] and  $\text{RH} = 80$  [%], while respectively 3.3 and 12.1  
 77 [ $\mu\text{g}/\text{m}^3(\text{air})$ ] of  $\text{NH}_3(\text{g})$  and  $\text{HNO}_3(\text{g})$  remain in the gas phase.

78 Compared to the solid case, the additional formation of  $64.7 - 55.2 \approx 9.5$  [ $\mu\text{g}/\text{m}^3(\text{air})$ ]  
 79  $\text{NH}_4\text{NO}_3$  corresponds to a change in RH from 50 to 80 [%]. Fig. 10.21 of SP2006 de-  
 80 picts the situation of the RH-dependent equilibrium partitioning. For comparison Fig. 2  
 81 (see line-points) and Fig. 3 (left part of the upper panels) reveals the situation for our  
 82 EQSAM4clim and the ISORROPIA II applications.

### 83 S1.3 EQSAM4clim algorithm: $\text{NH}_4\text{NO}_3$ -equilibrium

84 To provide a complete example for mixed solution cases with an analytical solution of  
 85 EQSAM4clim (Sec. 2.5), we consider Fig. 3 (Sec. S1.1–S1.2) in terms of the notation  
 86 of SP2006. For EQSAM4clim, we obtain the  $\text{NH}_4\text{NO}_3$ (*nro*) equilibrium concentration by  
 87 solving Eqs. (6–12), based on chemical domains (Table 2, Sec. 2.2) and the neutralization  
 88 reaction order (NRO, Table 3, Sec. 2.3).

#### 89 I. Single Solution, Dry/Wet Case (Fig. 3, upper panels)

90  
 91 For the single solution case shown in Fig. 3, we assume for the EQSAM4clim computa-  
 92 tions a total (gas+aerosol) cation and anion input concentration of 1 [ $\mu\text{mol}/\text{m}^3(\text{air})$ ], i.e.,  
 93 total ammonium  $[TA] = [\text{NH}_4^+]_{(nro,free)} = 1$  and total nitrate  $[TN] = [\text{NO}_3^-]_{(nro,free)} = 1$ .  
 94 For this sulfate neutral case (all other ions are zero), we apply domain D1. Solving  
 95 the NRO for D1 automatically yields only a single reaction, i.e., for  $\text{NH}_4\text{NO}_3$ , since all  
 96 other cation and anion products are zero, so that just one ion-pair combination can  
 97 exist. Considering the ion charge,  $[ZN] = [ZA] = 1$ , we can obtain from the prod-  
 98 uct  $[TA] \cdot [ZA]$  and  $[TN] \cdot [ZN]$  the corresponding maximum ammonium nitrate con-  
 99 centration  $[\text{NH}_4\text{NO}_3]_{(nro,max)} := \text{MIN}([TA] \cdot [ZA], [TN] \cdot [ZN]) = 1$  [ $\mu\text{mol}/\text{m}^3(\text{air})$ ],  
 100 which is possible for the input concentration with  $K_p(T, RH, Y) := 1$  (Sec. 2.5),  $T$   
 101 and  $RH$ . The temperature is fixed to  $T = 298.15$  K, the RH varies from  $RH = 30$   
 102 to  $RH = 100$  [%]. After solving the NRO, [TA] and [TN] are zero over the entire  
 103  $RH$ -range, since here the input concentrations are fixed to 1 [ $\mu\text{mol}/\text{m}^3(\text{air})$ ] for this  
 104 pure  $\text{NH}_4\text{NO}_3$  case (binary solution, upper left panel of Fig. 3). To solve a dry and  
 105 wet case, we again consider  $RH = 50$  [%] and  $RH = 80$  [%]. According to Table 1,  
 106 the RHD= 61.83 [%] for  $\text{NH}_4\text{NO}_3$  so that at  $RH = 50$  [%] only the gas-solid equi-  
 107 librium partitioning needs to be considered, i.e., (R-1), while at  $RH = 80$  [%] the  
 108 gas-liquid equilibrium partitioning, i.e., (R-2), is relevant. In EQSAM4clim we solve  
 109 the equilibrium in molal scale. At  $T = 298.15$  K and  $RH = 50$  [%], conversion of  
 110  $K_p(T) = 57.46$  [ $\text{ppbv}^2$ ] (Table 4) to the molal scale yields (with  $K_p/(RT/P)^2$ ), i.e.,  
 111  $57.46$  [ $\text{ppbv}^2$ ]  $\cdot 10^{-18}/(8.314409/101325$  [ $\text{m}^3(\text{air})/\text{mol}/\text{K}$ ]  $\cdot 298.15$  [ $\text{K}$ ]) $^2 = 57.46 \cdot 1.67^{-15} =$   
 112  $9.6 \cdot 10^{-14}$  [ $\text{mol}/\text{m}^3(\text{air})$ ] $^2$ . Solving Eqs. (6–12), we then obtain for the evaporative loss  
 113  $[x]$  [ $\mu\text{mol}/\text{m}^3(\text{air})$ ] of  $[\text{NH}_4\text{NO}_3]_{(nro,max)}$ :

114  
 115  $x = 0.5 \cdot \sqrt{(4 \cdot 9.6 \cdot 10^{-14})} = 0.31$  [ $\mu\text{mol}/\text{m}^3(\text{air})$ ], with  $[TA] = [TN] = 0$ . Thus, at  
 116  $RH = 50$  [%],  $\text{NH}_4\text{NO}_3]_{(s,nro)} = 1 - 0.31 \approx 0.69$  [ $\mu\text{mol}/\text{m}^3(\text{air})$ ], or  $0.69[\mu\text{mol}/\text{m}^3(\text{air})]$   
 117  $\cdot 80$  [ $\text{g}/\text{mol}$ ]  $\approx 55.2$  [ $\mu\text{g}/\text{m}^3(\text{air})$ ] for the total particulate matter (PM). For the aque-  
 118 ous phase at  $RH = 80$  [%], we analogously obtain  $\text{NH}_4\text{NO}_3]_{(aq,nro)}$ . According to the  
 119 above example (Sec. S1.2),  $K_{p,AN}(T = 298, RH = 80\%) = 57.5 \cdot 0.39 \approx 22$  [ $\text{ppbv}^2$ ], so  
 120 that we get;  $= 22 \cdot 1.67^{-15} = 3.7 \cdot 10^{-14}$  [ $\text{mol}/\text{m}^3(\text{air})$ ] $^2$  and  $x = 0.5 \cdot \sqrt{(4 \cdot 3.7 \cdot 10^{-14})}$   
 121  $\approx 0.19$  [ $\mu\text{mol}/\text{m}^3(\text{air})$ ]. This yields  $\text{NH}_4\text{NO}_3]_{(aq,nro)} \approx 0.81$  [ $\mu\text{mol}/\text{m}^3(\text{air})$ ], or for the  
 122 total PM  $\approx 0.81$  [ $\mu\text{mol}/\text{m}^3(\text{air})$ ]  $\cdot 80$  [ $\text{g}/\text{mol}$ ]  $\approx 64.6$  [ $\mu\text{g}/\text{m}^3(\text{air})$ ]. These values refer  
 123 respectively to the (upper) left and right panels of Fig. 3, and are close to the values of  
 124 ISORROPIA II, which are independently computed with a different approach.

#### 125 II. Mixed Solution, Dry/Wet Case (Fig. 3, lower panels)

126  
 127 For the mixed solution case shown in Fig. 3, we assume for the EQSAM4clim computa-  
 128 tions a total (gas+aerosol) cation and anion input concentration ( $[\mu\text{mol}/\text{m}^3(\text{air})]$ )

130 of total ammonium  $[TA] = [NH_4^+]_{(nro,free)} = 3$ , total nitrate  $[TN] = [NO_3^-]_{(nro,free)} = 1$ ,  
 131 and total sulfate  $[TS] = [SO_4^{2-}]_{(nro,free)} = 1$ . This sulfate case also falls into domain D1,  
 132 since other ions are zero. Solving the NRO for D1 yields two reactions. Considering the  
 133 ion charge,  $[ZN] = [ZA] = 1$  and  $[ZS] = 2$ , we can directly obtain from the NRO and  
 134 the products  $[TA] \cdot [ZA]$ ,  $[TN] \cdot [ZN]$  and  $[TS] \cdot [ZS]$  the corresponding maximum  
 135 concentrations of ammonium sulfate and ammonium nitrate, which is possible for the  
 136 input concentration with  $K_p(T, RH, Y) := 1$  (Sec. 2.5 and S1.3-I):

- 137 1.  $[TA] \cdot [ZA] = 3$  and  $[TS] \cdot [ZS] = 2$ :  
 138  $[(NH_4)_2SO_{4(nro,max)}] := MIN([3], [2]) = 1$
- 139 2.  $[TA = 3 - 2 = 1] \cdot [ZA = 1] = 1$  and  $[TN = 1] \cdot [ZN = 1] = 1$ :  
 140  $[NH_4NO_{3(nro,max)}] := MIN([1], [1]) = 1$

141 Extending our above example calculation (Sec. S1.3-I) to the mixture of  $NH_4NO_3$  of  
 142  $1 [\mu mol/m^3(air)]$  of each  $NH_4NO_3$  and  $(NH_4)_2SO_4$  (lower left panel of Fig. 3), we compute  
 143 the dry ( $RH = 50$  [%]) and wet ( $RH = 80$  [%]) case. For  $NH_4NO_3$ , the RHD= 61.83 [%]  
 144 and for  $(NH_4)_2SO_4$  the RHD= 79.97 [%] (Table 1), so that at  $RH = 50$  [%] again only  
 145 the gas-solid equilibrium partitioning needs to be considered. Note that mixed solution  
 146 effects described in Sec. 2.6 are not considered for the RHD in this example, but they  
 147 are considered for the gas-liquid and liquid-solid equilibrium partitioning and associated  
 148 aerosol water uptake examples presented in Sec. 3.

149 For the mixed solution case, the computation is similar to that discussed above  
 150 (Sec. S1.3-I), only the ionic strength factor needs to be included for the wet case. For the  
 151 dry case, the solid equilibrium concentration,  $NH_4NO_{3(s,nro)}$ , is identical, since  $Y := 1$   
 152 (the ionic strength correction factor is defined only for solutions). The total dry aerosol  
 153 mass therefore is the sum of the  $NH_4NO_{3(s,nro)}$  (from above) and  $(NH_4)_2SO_{4(s,nro)}$  masses,  
 154 i.e.,  $PM \approx 55.2 + 132.2 = 187.4 [\mu g/m^3(air)]$ . For the aqueous case, we obtain  $Y$  from  
 155 Eq. (4) (as used for Eq. 5), i.e., we obtain for  $1 [\mu mol/m^3(air)]$  of each,  $NH_4NO_{3(aq,max,nro)}$   
 156 and  $(NH_4)_2SO_{4(aq,eq)}$ ,  $Y = \frac{1}{1+3 \cdot 1} = 0.25$ . Using further the above (Sec. S1.2) value  
 157 for  $\mu_{AN}(a_w = 0.8) \approx 10 [mol_{AN}/kg(H_2O)]$  (Fig. A1), we compute the solute mass frac-  
 158 tion again from Eq. (A1) as  $\chi_{AN}(a_w = 0.8) = (\frac{1}{0.08 \cdot 10} + 1)^{-1} = 0.44$ . Then, Eqs. (3)  
 159 and (5) yield  $COEF(RH, Y) = 2 \cdot 0.44^2 \approx 0.39$  and  $Y^{0.8} = 0.25^{0.8} = 0.33$ , so that  
 160  $K_{p,AN}(T = 298, RH = 80\%, Y = 0.25) = 57.5 \cdot 0.39 \cdot 0.33 = 7.4 [ppbv^2]$ , or  $7.4 \cdot 1.67^{-15}$   
 161  $= 1.24 \cdot 10^{-14} [mol/m^3(air)]^2$ . Solving Eqs. (6–12), we then again obtain for the evapo-  
 162 rative loss  $[x] [\mu mol/m^3(air)]$  of  $[NH_4NO_{3(nro,max)}]$ :

163  $x = 0.5 \cdot \sqrt{(4 \cdot 1.24 \cdot 10^{-14})} \approx 0.11 [\mu mol/m^3(air)]$ , with  $[TA] = [TN] = 0$ . Thus,  
 164 at  $RH = 80$  [%],  $NH_4NO_{3(aq,nro)} = 1 - 0.11 \approx 0.89 [\mu mol/m^3(air)]$ , or for the total (dis-  
 165 solved)  $PM \approx 0.89 [\mu mol/m^3(air)] \cdot 80 [g/mol] + 132.2 [\mu g/m^3(air)] = 203.4 [\mu g/m^3(air)]$ .  
 166 These values refer to the (lower) left and right panels of Fig. 3, respectively, and are also  
 167 close to the results of ISORROPIA II, despite the distinctly different approaches.

## 168 S2 Computational algorithm of EQSAM4clim

169 The EQSAM4clim computational algorithm is summarized as follows (see Fig. S2-S1):

- 170 • EQSAM4clim (v09), described in Sec. B, considers the salt compounds listed in Ta-  
 171 ble 1. To calculate the gas-liquid-solid partitioning, a pre-calculated (constant)  $\nu_i$

coefficient is used for each compound (ion-pair), which is obtained from a small set of thermodynamic data: stoichiometric coefficient  $\nu_s$  [-], the ion-pair charge  $Z_s$  [-], the single solute parameter  $\nu_i$  [-], the mass fraction solubility  $W_s$  [%], the molar mass  $M_s$  [ $kg/mol$ ], the density  $D_s$  [ $kg/m^3$ ], the RHD( $T_o$ ) [-] at reference temperature  $T_o = 298.15$  [ $K$ ] and the corresponding temperature coefficients,  $T_{coef(RHD)}$  [-]. For all salt compounds,  $\nu_i$  has been pre-determined with the bi-section method by the procedure of solving Eq. (5b) of M2012 (Eq. A6 in Appendix A4), using measurements of  $W_s$ -RHD( $T_o$ ) (single data pairs) at  $T_o$ , which are listed with  $\nu_i$  in Table 1. The required RHD values, including T-coefficients, have been taken from ISORROPIA II for a consistent comparison (Fountoukis and Nenes, 2007). All other data of Table 1 have been taken from the CRC Handbook of Chemistry and Physics (2006).

- The EQSAM4clim algorithm starts with the assignment of two internal loop parameters: An outermost loop, considering e.g., vertical model levels, and an innermost vector loop for e.g., the longitude-latitude grid box that contains the input-data for a given time-step. Both loops are scalable and can be externally determined depending on the climate model set-up, e.g., to best match the cache of the compute nodes. The consideration is optional and can be controlled in the subroutine call. The actual computations are structured in blocks, which are fully sequential. Each computational block has its own vector loop with the compound specific logic around it, so that loops can be fully optimized by the compiler and iterations between different computational blocks are avoided. All computational blocks are within an outermost loop (for this version).
- The first two computational blocks (out of 15) assign the T [ $K$ ] and RH [0–1] data, as well as the lumped cations and anion concentrations [ $mol/m^3(air)$ ]. Further, the total cation and anion concentration charge is computed and a logical switch for each compound is defined. Thus, we assume that a compound can be formed only, if the product of the required cation and anion concentration is non-zero. This compound specific flag is subsequently used to skip the computation of individual compounds, which may not be present at the considered model time step. The flag is applied to all computational blocks which have an outer compound loop. In case all cation and anion concentrations are zero, i.e., the total cation charge equals (or is below) REALZERO = tiny(0.dp) (with dp = SELECTED\_REAL\_KIND(12,307)), none of the compounds could form and we therefore skip all computations. Depending on the EMAC model set-up and the number of compounds considered, this may happen for instance in remote locations such as the upper stratosphere. Both options are merely included to minimize the overall computational burden.
- To further minimize the CPU time, the next computational block (3) defines:
  - Whether solids are excluded or included, i.e., the hysteresis loop. The criteria depend on the presence of aerosol water of the previous time step. In case aerosol water is not present, the aerosol is assumed to be dry and the water uptake is calculated based on RH and RHD thresholds. Otherwise, gas-liquid partitioning is considered and the water uptake is calculated without RHD thresholds, assuming the aerosol phase to be metastable.
  - The domain that needs to be considered. Similar to ISORROPIA II, we consider a domain approach (Sec. 2.2). But the approach used here only depends

218 on the input concentration ratio of total cations (tCAT) to total sulfate anions  
219 (tSO<sub>4</sub>), which is more elementary compared to the domain approach used in  
220 ISORROPIA II and is similar to the one used in the original EQSAM code  
221 (Metzger et al., 2002). Table 2 lists the domains used to characterize the  
222 potential sulfate aerosol neutralization levels.

- 223 • The next two computational blocks initialize the internal arrays, including all out-  
224 put fields, while block (5) defines the neutralization reaction order for all com-  
225 pounds that may form for a given domain during the cation-anion neutralization.  
226 The compound’s indices are ranked according to a preferred neutralization (from  
227 left to right). The domain dependent neutralization order is shown in Table 3.
- 228 • Computational block (6) solves the compound’s solute molality  $\mu_s$  from Eq. (A3),  
229 by optionally including the Kelvin-term. To avoid iteration, we take a two-step  
230 approach / approximation (see Appendix B):

- 231 – Step one:  $K_e = 1$ , and  $B = 0$  to obtain the initial  $\mu_s$  from Eq. (A3).
- 232 – Step two, repeated three times:  $\mu_s$  from previous iteration is used to calculate  
233  $K_e$  from Eq. (A7),  $\chi_s$  from Eq. (A1),  $B$  from Eq. (A4). Then a new  $\mu_s$  is  
234 obtained from Eq. (A3).

235 Note that we sequentially solve the equations three times, whereby we only loop  
236 over those compounds of Table 1 that are allowed to form and those compounds  
237 that have a non-zero input ion-pair concentration (determined by block 2).

- 238 • The next computational block (7) calculates the temperature dependency of the  
239 RHD from Eq. (A5) and optionally considers the Kelvin effect according to Eq. (A7).
- 240 • In computational block 8, the actual cation-anion neutralization reactions are solved  
241 assuming chemical equilibrium. Based on the pre-defined reaction order the input  
242 cation and anion concentrations are balanced (neutralized) by looping over all com-  
243 pounds those cation-anion product is above REALZERO. As a result, the cation  
244 and anion concentrations subsequently decrease in favor of the concentrations of  
245 the corresponding compounds, independent of any solvent and solute activity.  
246 Within the same loop, we calculate the total solute activity and store the RHD val-  
247 ues only for the compound’s that have a non-zero concentration. This information  
248 is subsequently used to analytically solve the liquid-solid partitioning.
- 249 • Computational block 9 approximates the mixed solution RHD from Eqs. (18-21).
- 250 • Thus far, all compounds have been treated as non-volatile and are assumed to reside  
251 in the aqueous phase. Computational block (10) solves the gas-liquid or gas-solid  
252 partitioning for the two semi-volatile compounds, NH<sub>4</sub>NO<sub>3</sub> and NH<sub>4</sub>Cl, that may  
253 be present in the sulfate neutral / poor (D1) domain (Sec. 2.4). Within one loop,  
254 Eqs. (2-5) are computed and the reactions (Eq. R-2) are sequentially solved. In case  
255 the RH is below the semi-volatile compound’s RHD, Eq. 1 is used.
- 256 • The liquid-solid partitioning is calculated for all salt compounds in computational  
257 block 11 from the weighted mixed solution approach, Eqs. (13-21), described in  
258 Sec. 2.6. Each compound is treated as solid (instantaneously precipitated from the

- 259 solution) in case the RH is below the compound's RHD (binary solution), or in case  
 260 of mixed solutions below the weighted RHD.
- 261 • Within computational block 12 all partial aerosol water mass are calculated from  
 262 Eq. (22) for those compounds with a non-zero aqueous phase concentration. The  
 263 total water mass is obtained from the sum of all partial water masses (Sec. 2.7).
  - 264 • Computational block 13 estimates the final  $H^+$  concentration [ $mol$ ] from the dif-  
 265 ference of the total anion and cation concentrations. Within EMAC/GMXe the  
 266  $H^+$  concentration is recalculated for both EQSAM4clim and ISORROPIA II to ac-  
 267 count for the changes in the aerosol precursor gas concentrations, which may result  
 268 from the size-dependent condensation of  $HNO_3$ ,  $HCl$  and  $NH_3$  and  $H_2SO_4$  on the  
 269 pre-existing aerosol surfaces (see Pringle et al., 2010a).
  - 270 • Finally, the residual gases are calculated within computational block 14 from the  
 271 remaining ion concentrations based on the implicit assumptions that: (i) Unneu-  
 272 tralized  $NH_4^+$  will instantaneously be fully vaporized to yield  $NH_3$ , unneutralized  
 273  $NO_3^-$  yields  $HNO_3$  and unneutralized  $Cl^-$  yields  $HCl$ . (ii) In addition, unneutral-  
 274 ized  $SO_4^{2-}$  is assumed to yield  $H_2SO_4$ , which is however treated as non-volatile;  
 275 vaporization of  $H_2SO_4$  is considered within GMXe (Brühl et al., 2012).  $H_2SO_4$   
 276 contributes to the water uptake (assuming the solute molality of  $(NH_4)_3H(SO_4)_2$ ).
  - 277 • The last computational block (15) prepares the model output, which is user specific  
 278 and can be individually extended or configured to write out all aerosol properties.

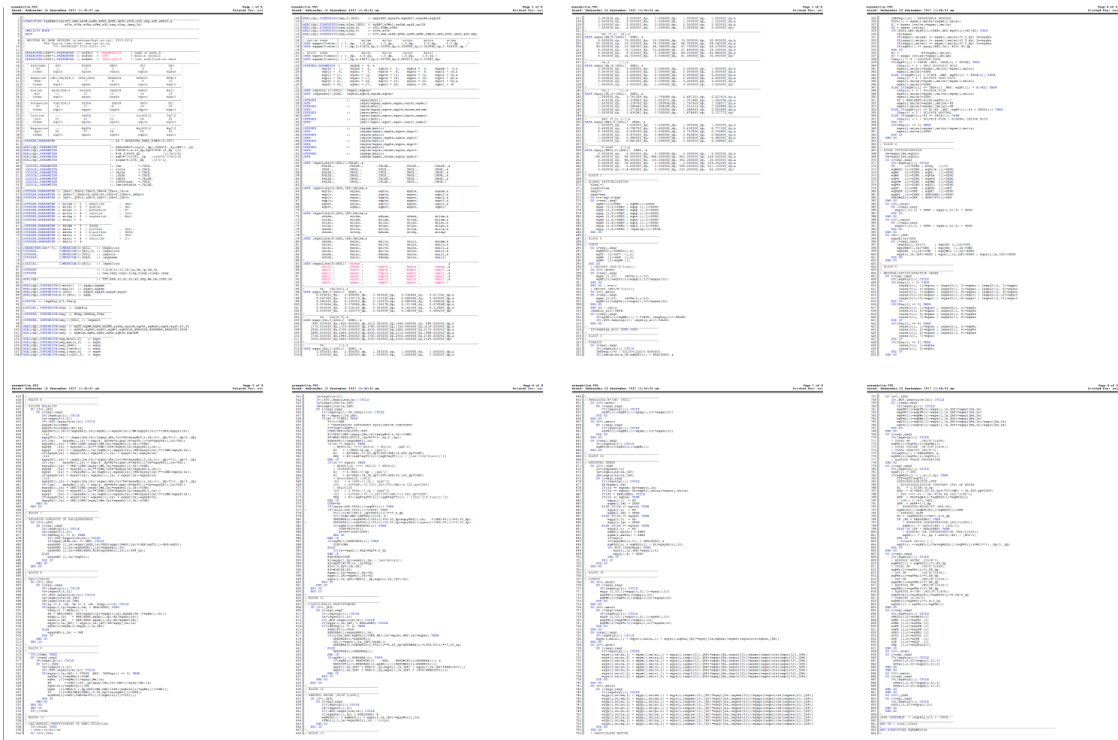


Figure S1: EQSAM4clim computational algorithm (code length overview, no details).



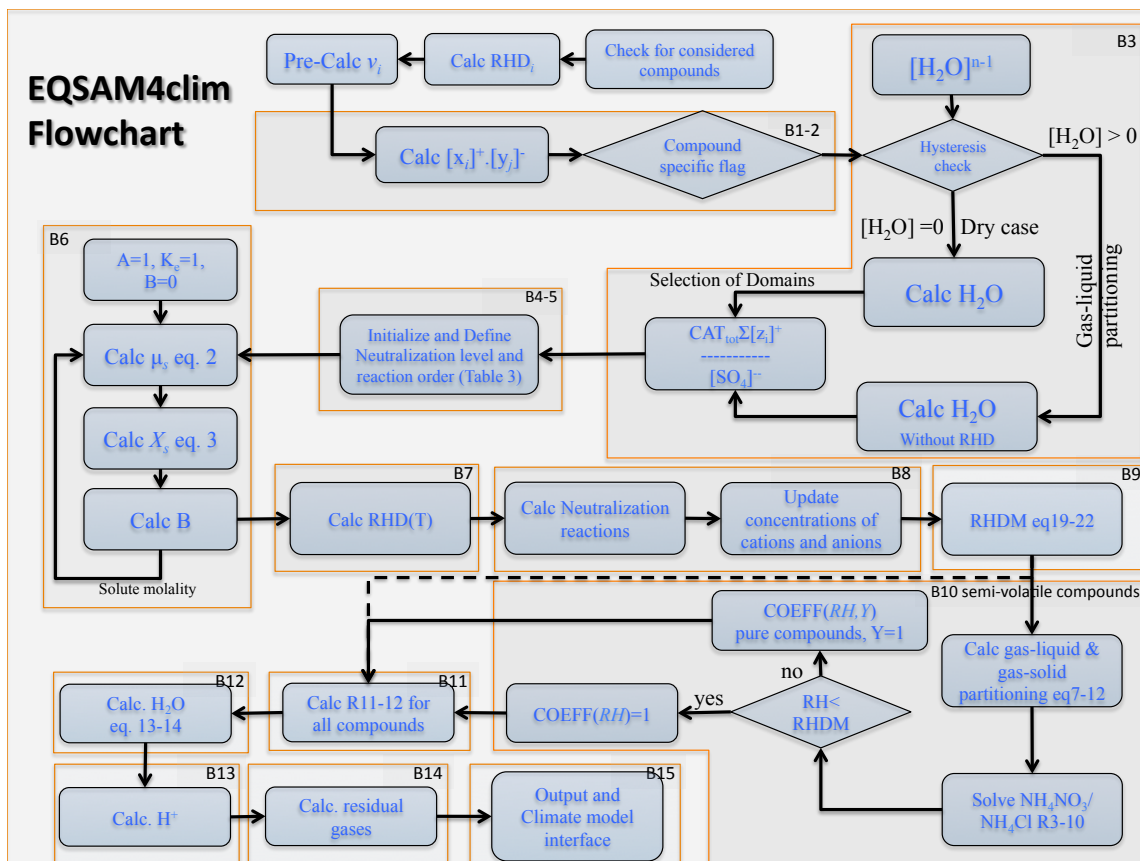


Figure S2: EQSAM4clim flowchart.

## 279 **S3 Extended Applications**

280 This section extends/complements the results shown in Sec. 3:

- 281 1. Fixed solute concentrations (9 cases): ISORROPIA II and E-AIM  
282 (see main text, Sec. 3.1)
- 283 2. Variable ammonia concentration: ISORROPIA II and Seinfeld and Pandis (2006)  
284 (see main text, Sec. 3.2)
- 285 3. Variable solute concentrations (20 cases): ISORROPIA II and EQUISOLV II  
286 (see main text, Sec. 3.3)
- 287 4. Field observations (MINOS campaign, 184 cases): ISORROPIA II  
288 (see main text, Sec. 3.4)

### 289 **S3.1 Fixed solute concentrations**

290 Figure S3 extends the aerosol water mass calculations shown in Figure 4 (see Sec. 3.1) to 9  
291 binary and mixed solution cases with fixed aerosol concentrations. The results are based  
292 on the full gas-liquid-solid partitioning and compare the calculations of EQSAM4clim  
293 with ISORROPIA II and E-AIM, with each (dry) compound concentration fixed to  
294  $1 [\mu\text{mol}/\text{m}^3(\text{air})]$ . The panels of Figure S3 show (from left to right, top-down):

- 295 • single solute solutions:  
296 (1.) NaCl; (2.)  $(\text{NH}_4)_2\text{SO}_4$ ; (3.)  $\text{NH}_4\text{NO}_3$ ;
- 297 • mixed solutions:  
298 (4.)  $\text{NH}_4\text{HSO}_4 / (\text{NH}_4)_3\text{H}(\text{SO}_4)_2$ ;  
299 (5.)  $\text{NaHSO}_4 / \text{Na}_3\text{H}(\text{SO}_4)_2$ ;  
300 (6.)  $\text{NH}_4\text{NO}_3 - (\text{NH}_4)_2\text{SO}_4$ ;  
301 (7.)  $\text{NaNO}_3 - \text{NaCl} / \text{NaCl}$ ;  
302 (8.)  $(\text{NH}_4)_2\text{SO}_4 - \text{NH}_4\text{Cl} - \text{Na}_2\text{SO}_4$ ;  
303 (9.)  $\text{NH}_4\text{NO}_3 - (\text{NH}_4)_2\text{SO}_4 - \text{NH}_4\text{Cl} - \text{Na}_2\text{SO}_4$

304 The large panels show the aerosol water mass predictions for the RH range = 50 – 97 [%],  
305 while the small inserted panels expand the range to RH = 95 – 99.5 [%].

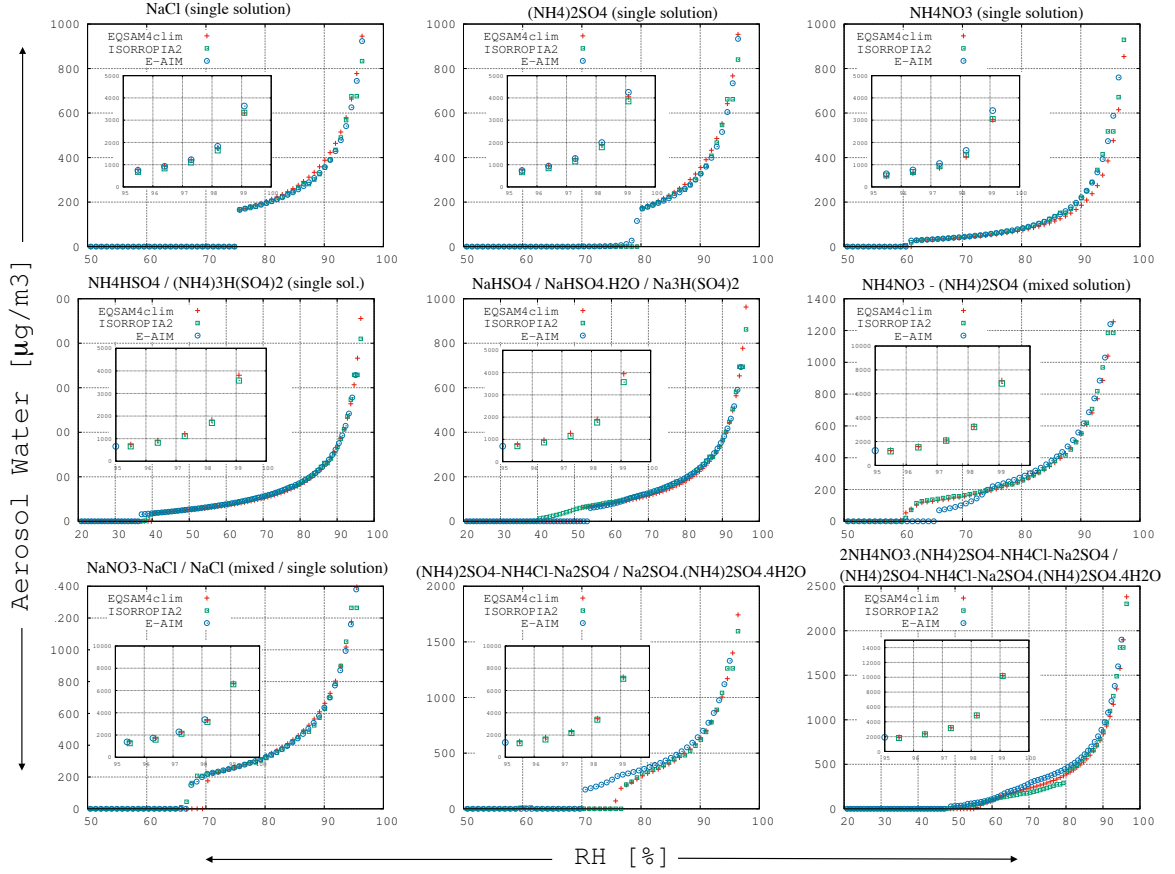


Figure S3: Extension of Figure 4 (main text): The bulk comparison of the total aerosol water mass,  $m_{w,mix} [kg/m^3(air)]$  obtained by Eq. (22) for EQSAM4clim, is shown for various single and mixed solutions. The dry concentration of each compound is fixed to  $1 [\mu mol/m^3(air)]$  at  $T = 298.15 K$ . Results of EQSAM4clim (red crosses) and ISORROPIA II (green squares) are shown for  $RH = 50 - 97 [\%]$  (large panels) and for the  $RH = 95 - 99.5 [\%]$  (small panel). The results of E-AIM (web version) (blue circles) are included for comparison. The mixed solution RHD has been obtained for EQSAM4clim from Eq. (13–22) and are based on measured MDRH values for ISORROPIA II. The mutual deliquescence range of EQSAM4clim and ISORROPIA II (described in Sec. 2.6) differ from those of AIM (web version: <http://www.aim.env.uea.ac.uk/aim/aim.php>). Each panel is shown in the following for better reading.

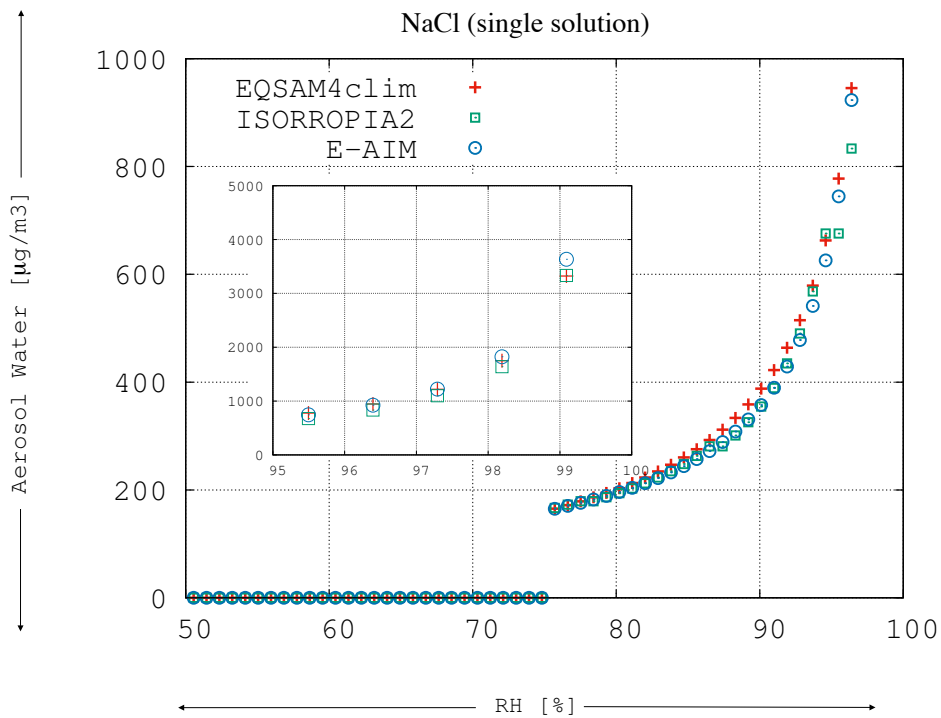


Figure S3.1: Panel 1 of Figure S3 (Supplement).

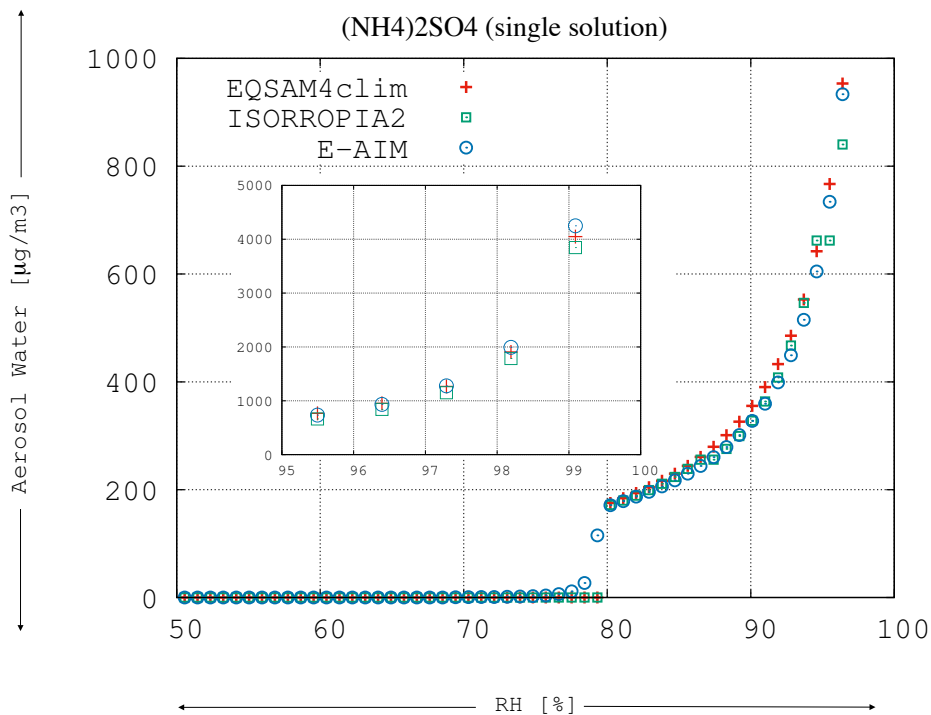


Figure S3.2: Panel 2 of Figure S3 (Supplement).

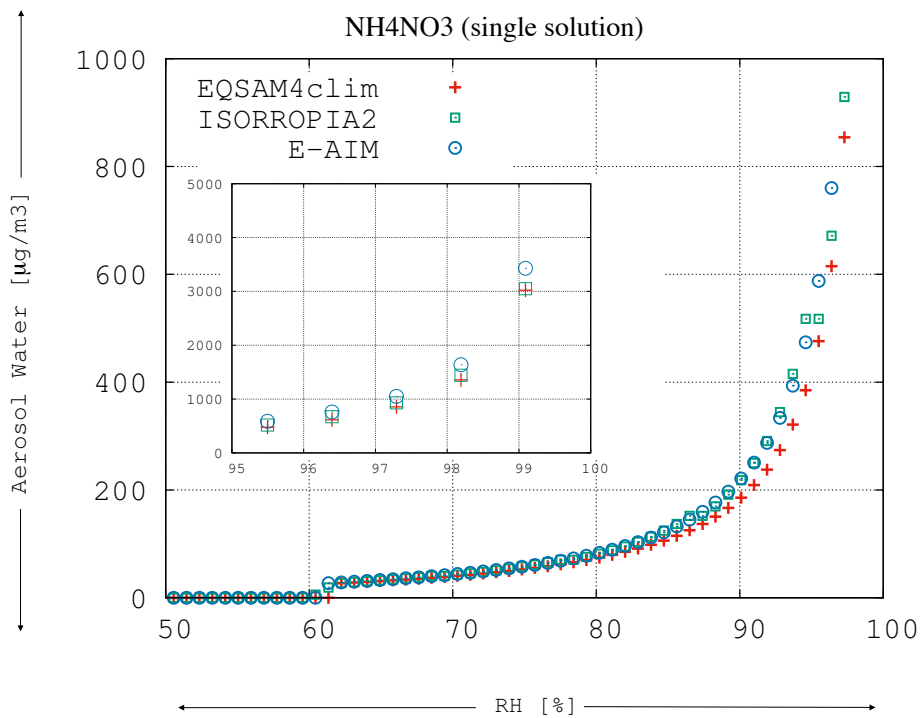


Figure S3.3: Panel 3 of Figure S3 (Supplement).

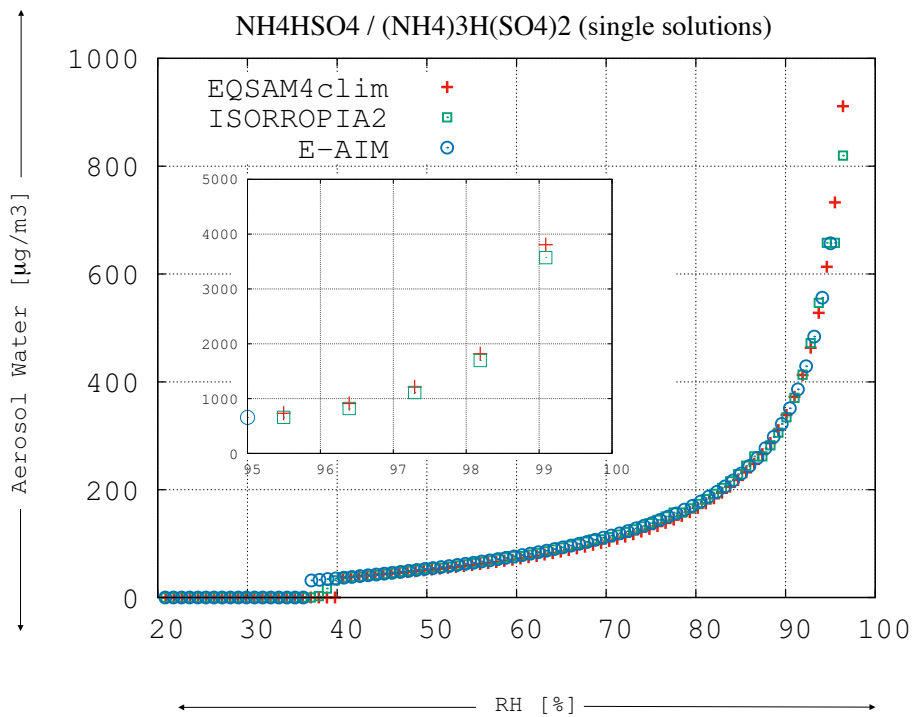


Figure S3.4: Panel 4 of Figure S3 (Supplement).

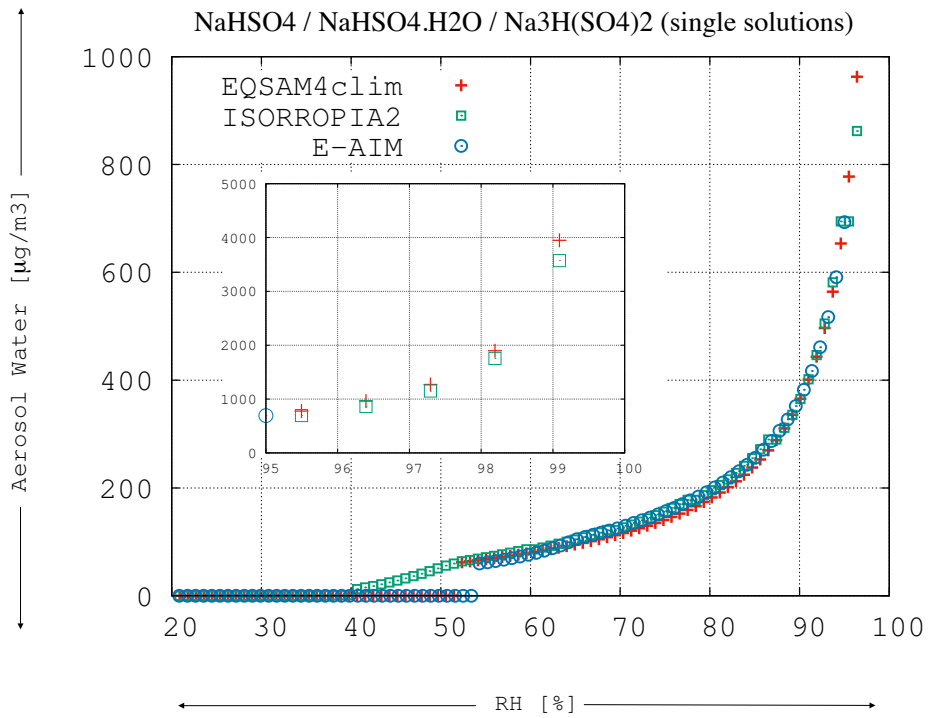


Figure S3.5: Panel 5 of Figure S3 (Supplement).

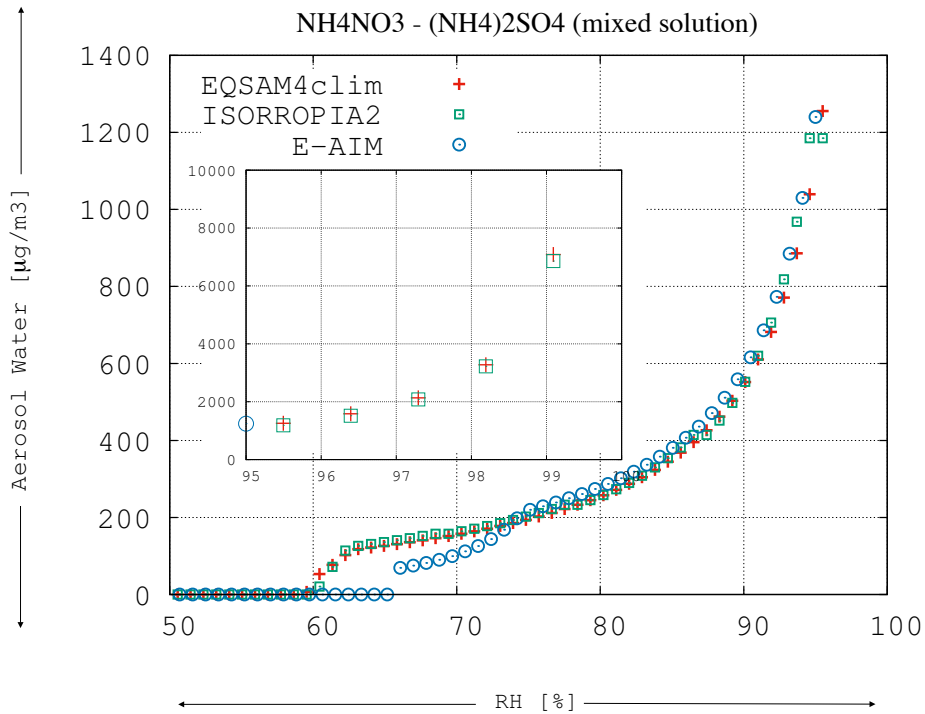


Figure S3.6: Panel 6 of Figure S3 (Supplement).

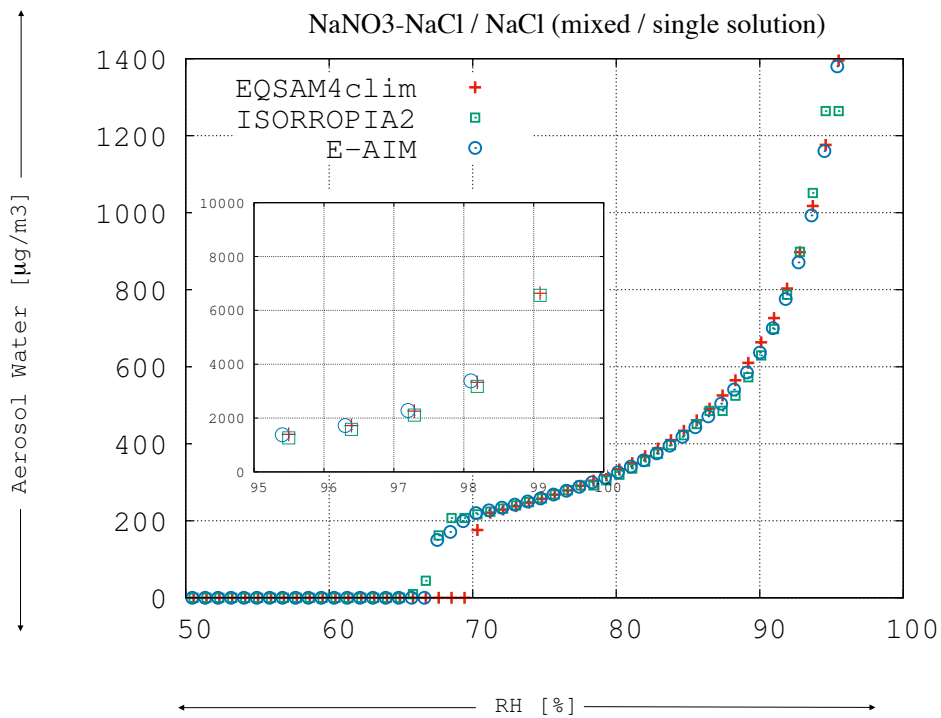


Figure S3.7: Panel 7 of Figure S3 (Supplement).

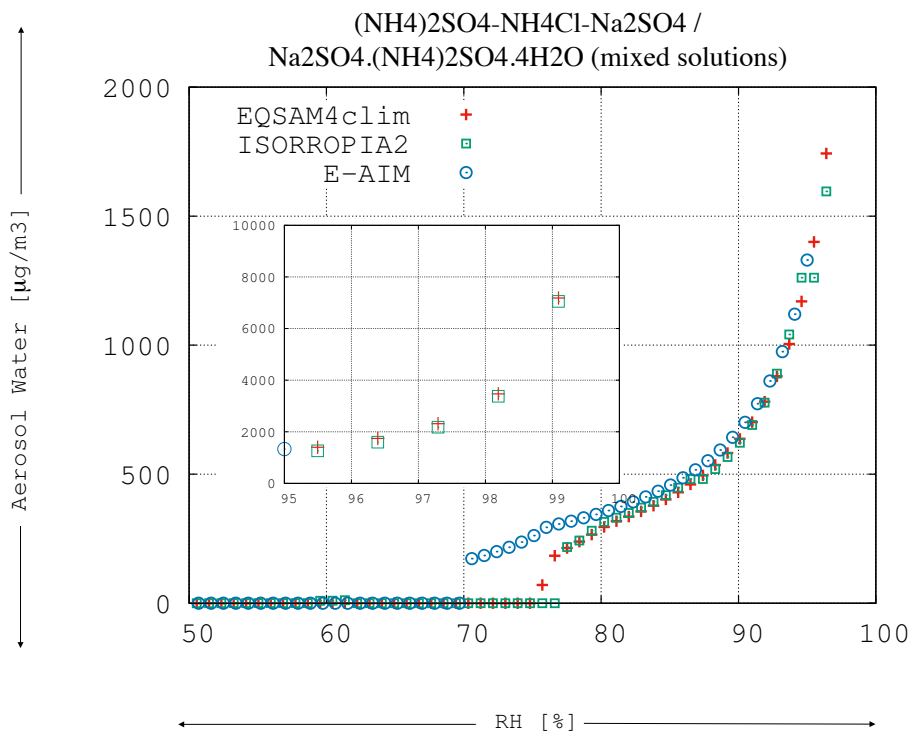


Figure S3.8: Panel 8 of Figure S3 (Supplement).

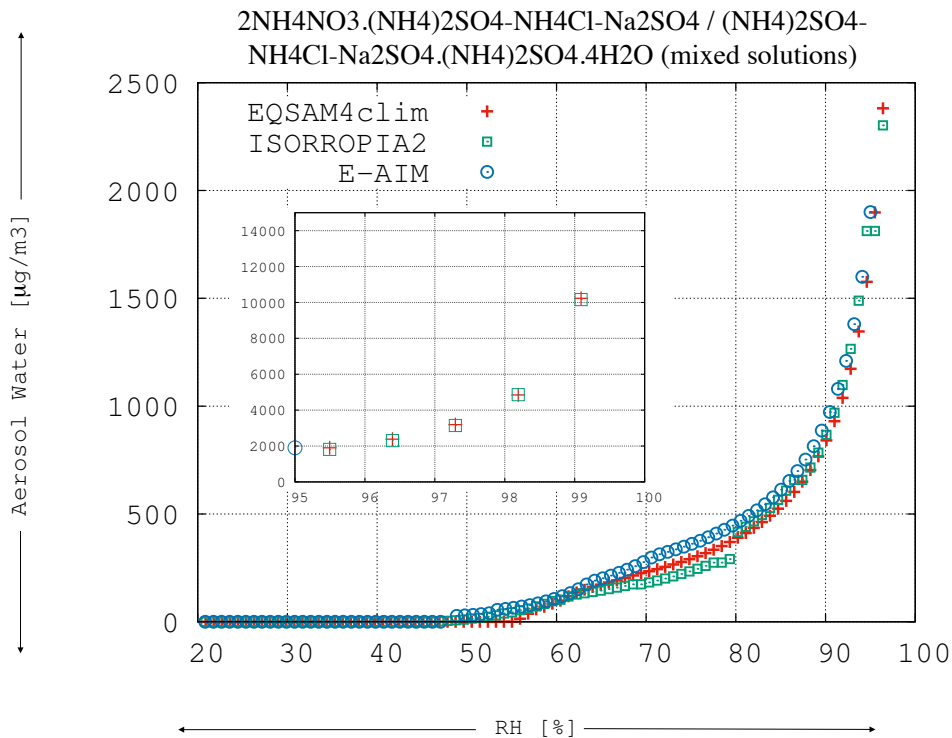


Figure S3.9: Panel 9 of Figure S3 (Supplement).

### 306 S3.2 Variable $\text{NH}_3$ concentration – SP2006

307 Figure S4 extends the Fig. 5 (main text) to bi-sulfate and sulfuric acid. Both, the  
 308 gaseous uptake of  $\text{NH}_3$  and  $\text{HNO}_3$  on saturated solutions and the weak dissociation of,  
 309 e.g.,  $\text{H}_2\text{SO}_4$  and  $\text{HSO}_4^-$ , are not considered for EQSAM4clim (see Sec. S2). Therefore  
 310 differences occur for bi-sulfate, sulfate and water in the concentration range of ammonia,  
 311 i.e., within  $2 - 4 \text{ } [\mu\text{g}/\text{m}^3(\text{air})]$ . At lower ammonia concentrations, where the sulfates are  
 312 less neutralized, the bi-sulfate concentration increases and the sulfate concentration ac-  
 313 cordingly decreases, until only free sulfuric acid exists. Note that the differences between  
 314 EQSAM4clim and ISORROPIA II are for ammonia concentrations below  $2 \text{ } [\mu\text{g}/\text{m}^3(\text{air})]$   
 315 only a matter of naming definition – the version of ISORROPIA II used considers all  
 316 unneutralized sulfate simply as sulfate, an output variable sulfuric acid does not exist,  
 317 since sulfuric acid has such a low vapor pressure that it practically only exists in the  
 318 aerosol phase. EQSAM4clim has an option to treat it either way.



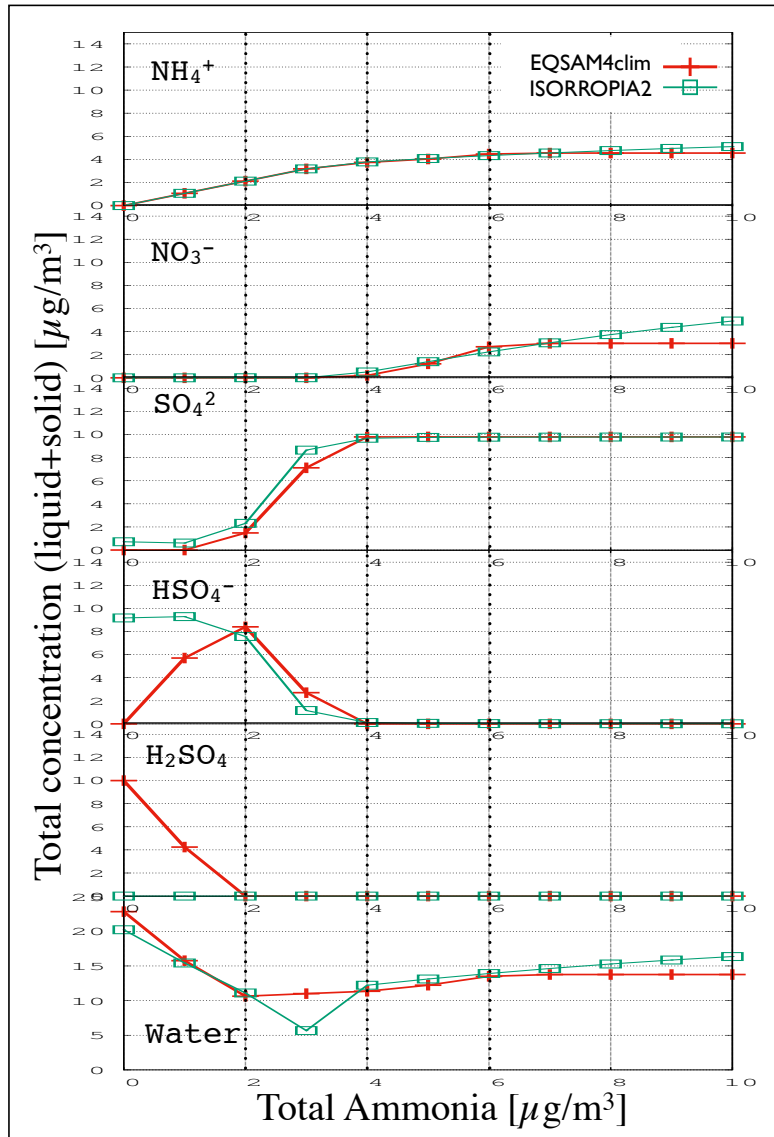


Figure S4: Extension of Figure 5 (main text): Mixed solution composition of  $\text{NH}_4\text{NO}_3$  and  $(\text{NH}_4)_2\text{SO}_4$  as a function of total ammonia at  $T = 298.15$  [K] and  $RH = 70$  [%], as defined in SP2006 for their Figure 10.23.  $[\text{TS}] = [\text{TN}] = 10$  [ $\mu\text{g}/\text{m}^3(\text{air})$ ] showing EQSAM4clim (red crosses) and ISORROPIA II (green squares). Each panel is shown in the following for better reading.

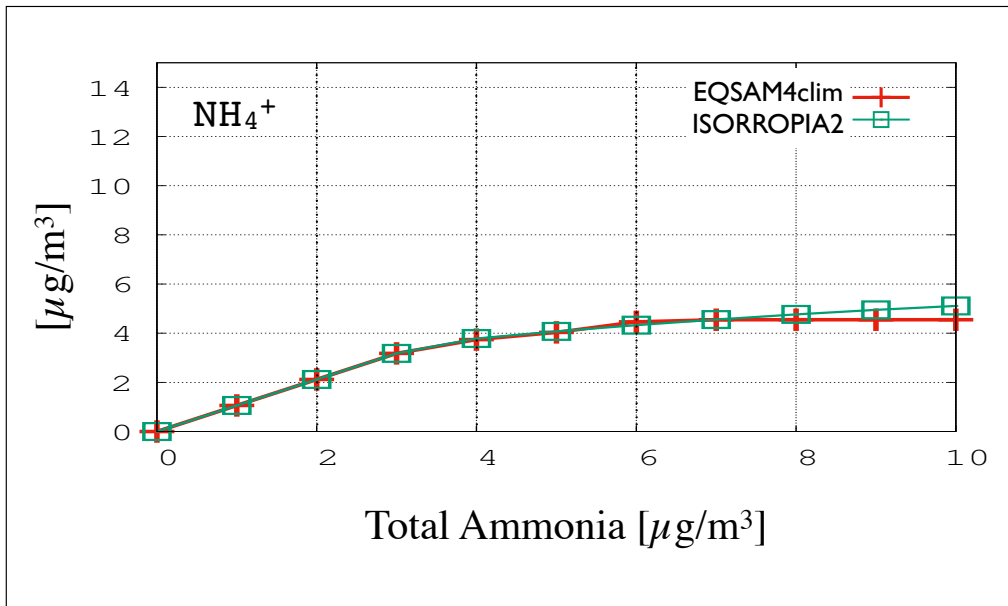


Figure S4.1: Panel 1 of Figure S4 (Supplement).

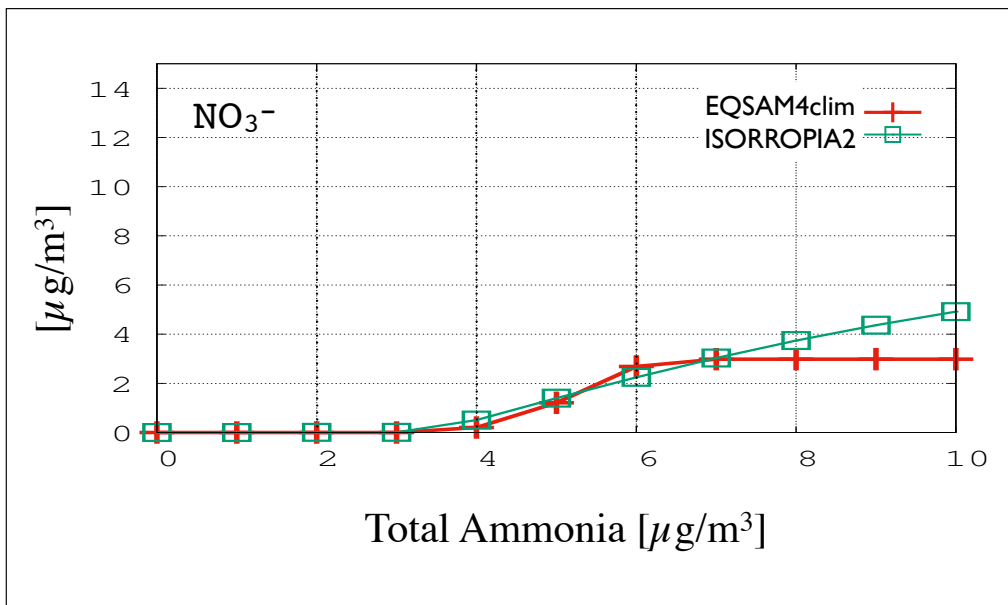


Figure S4.2: Panel 2 of Figure S4 (Supplement).

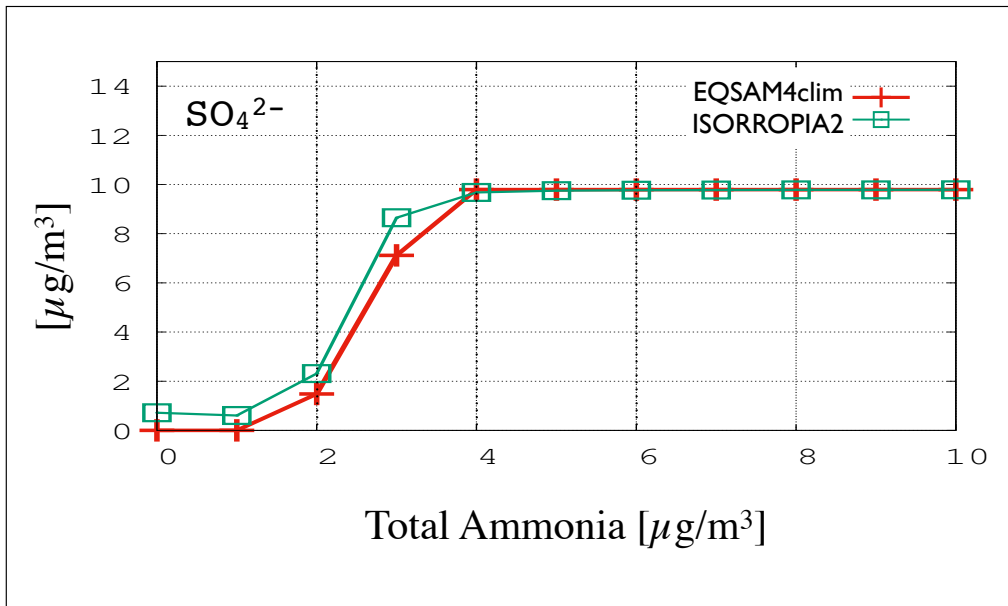


Figure S4.3: Panel 3 of Figure S4 (Supplement).

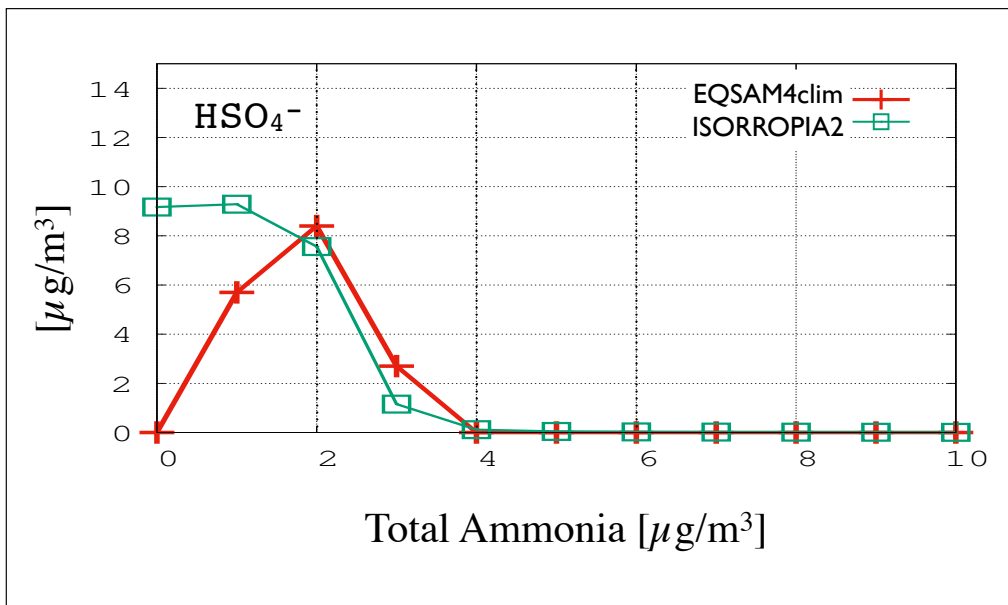


Figure S4.4: Panel 4 of Figure S4 (Supplement).

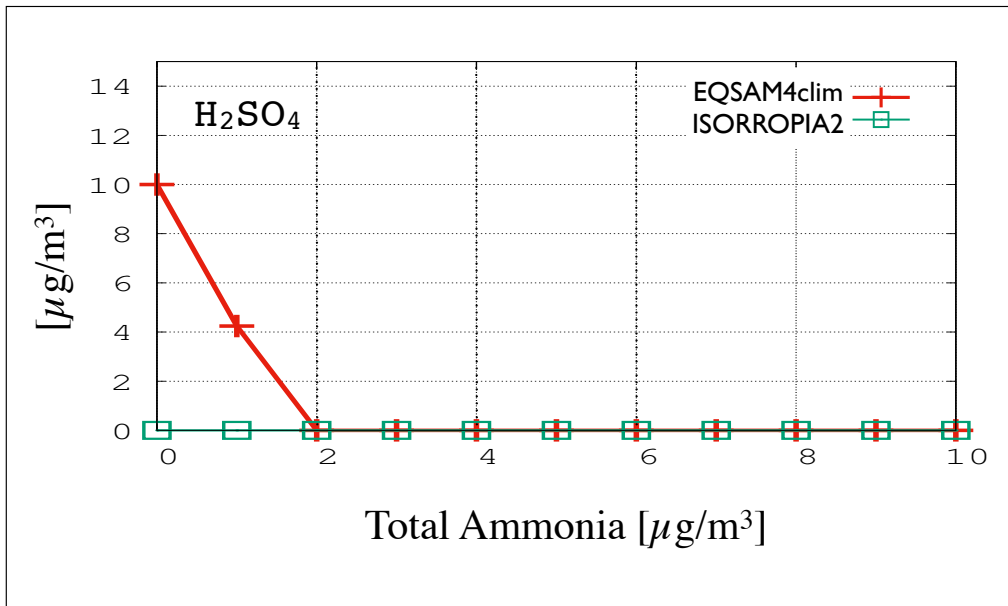


Figure S4.5: Panel 5 of Figure S4 (Supplement).

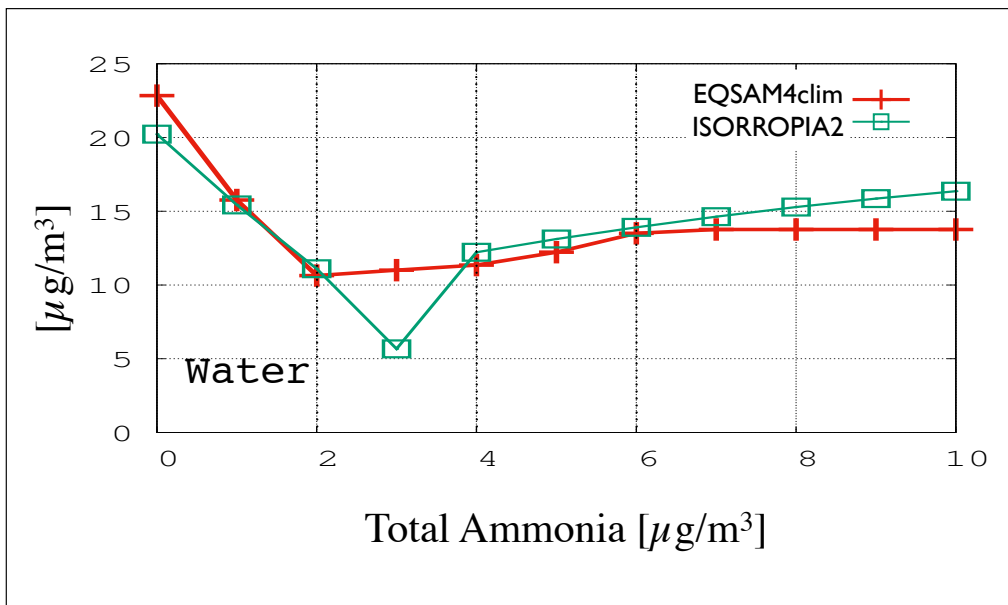


Figure S4.6: Panel 6 of Figure S4 (Supplement).

### 319 S3.3 Variable solute concentrations (20 cases)

320 Extension of Figure 6 and 7 to 20 aerosol composition cases. Cases 1–5 refer to the sulfate  
 321 very rich regime, cases 6–10 to sulfate rich, and 11–20 to sulfate neutral and poor regimes  
 322 (see Sec. 2.2). The concentrations of all aerosol components only depend on fixed molar  
 323 ratios with respect to the total sulfate concentration, which is fixed to 20  $[\mu\text{g}/\text{m}^3(\text{air})]$   
 324 for all 20 cases. The ratios are shown in Table 3 of Xu et al. (2009). Note that some of  
 325 the cases are the same as in the model inter-comparison of Zhang et al. (2000), so that  
 326 a direct comparison can be made to a wider range of equilibrium models, including AIM  
 327 (the case number in the parenthesis in Table 3 of Xu et al., 2009, refers to the cases in  
 328 the study by Zhang et al., 2000). Here, Figures S5–S7 show the corresponding results  
 329 of EQSAM4clim, ISORROPIA II and EQUISOLV II for these 20 cases as a function of  
 330 RH: 10, 20, 30, 40, 50, 60, 70, 80, 90, 95 [%]. The aerosol composition is calculated for each  
 331 model from the gas-liquid-solid equilibrium partitioning, assuming deliquescence.

332 Figure S5 shows for the cases 1-20 (from left to right and top to bottom), the bulk  
 333 aerosol water mass as a function of RH at  $T = 298.15 \text{ [K]}$ . Fig. S6 shows the corresponding  
 334 solid particulate matter (cases 11-20 in panels 1-10), panels 11-20 show the corresponding  
 335 total dry particulate matter (PM), i.e., the sum of the liquid and solid aerosol mass  
 336 (without aerosol water). Panels 1-10 of Fig. S7 show the total aerosol nitrate, while the  
 337 panels 11-20 the aerosol ammonium concentration (both show cases 11-20).

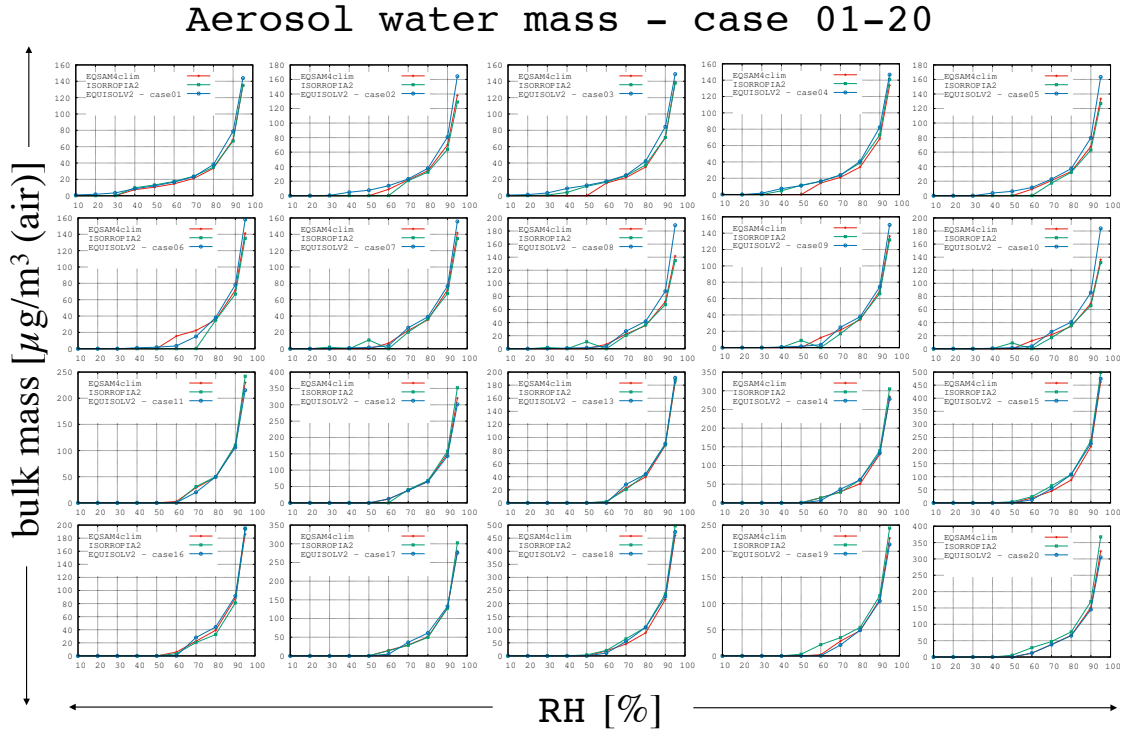


Figure S5: Extension of Figure 6 (main text): Bulk aerosol water mass as a function of RH for various sulfate molar ratios, fixed for the entire RH range (at constant  $T = 298.15 \text{ K}$ ). Only the dry concentration ratio varies from case to case to match the domains of Table 2. The 20 aerosol composition cases refer to Table 3 of Xu et al. (2009). A subset of four panels is shown in the following for better reading.

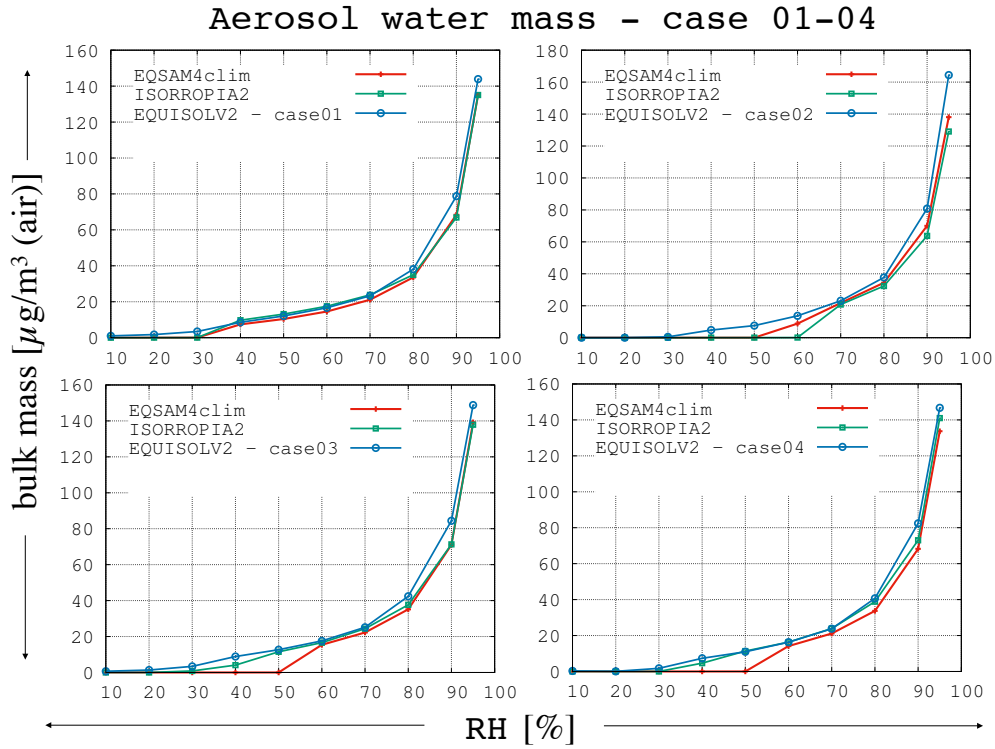


Figure S5.1: Case 1-4 of Figure S5 (Supplement).

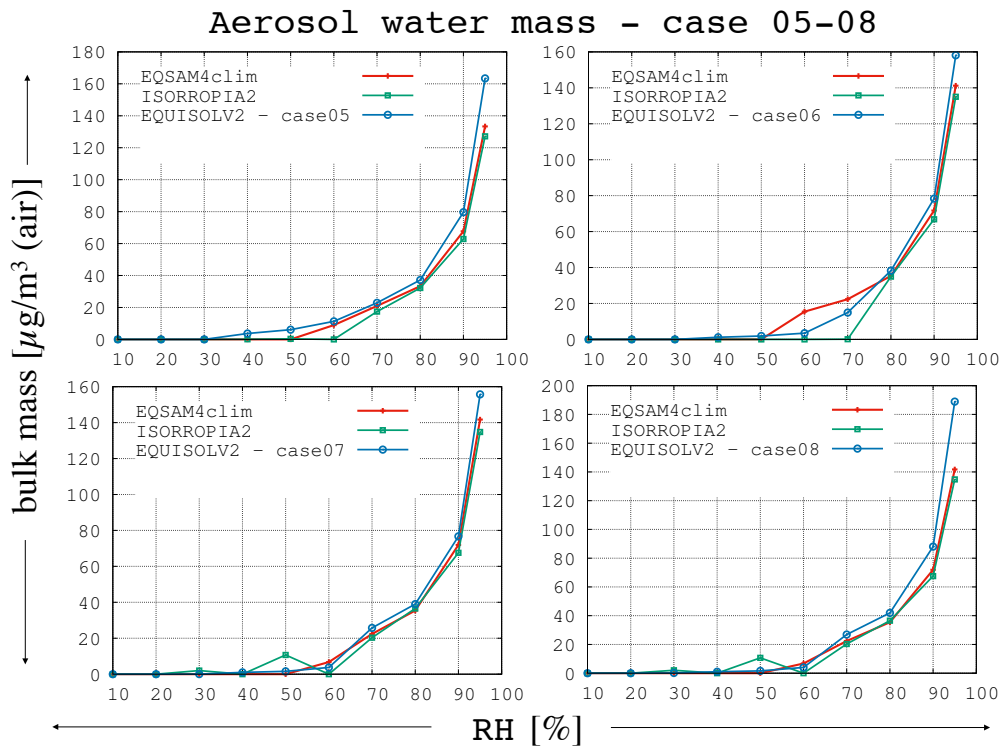


Figure S5.2: Case 5-8 of Figure S5 (Supplement).

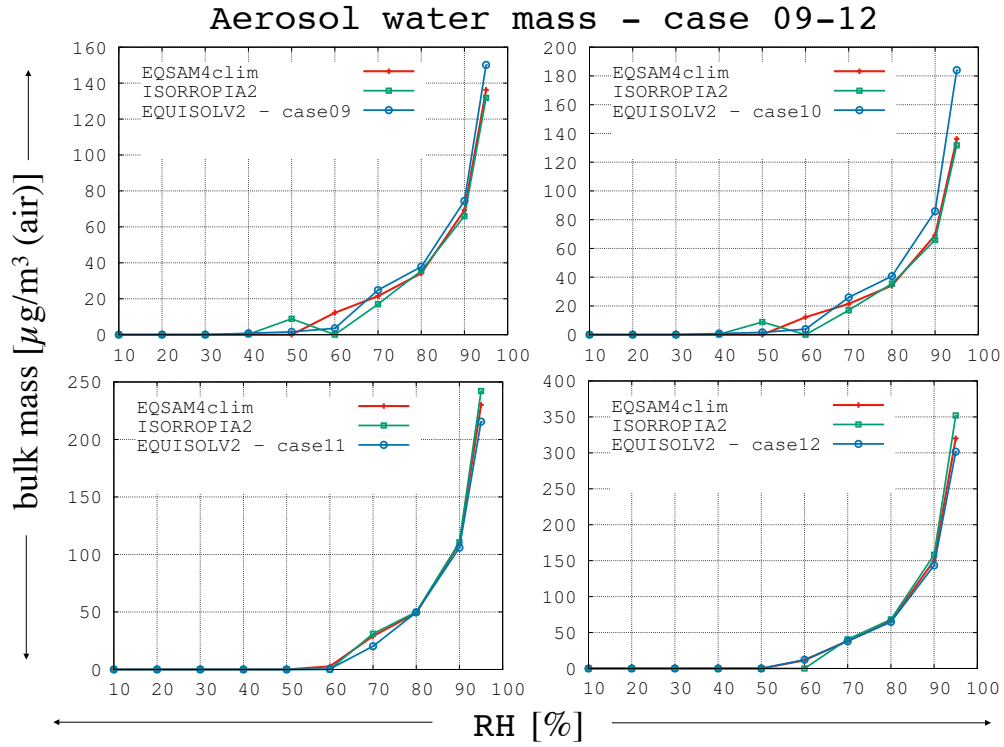


Figure S5.3: Case 9-12 of Figure S5 (Supplement).

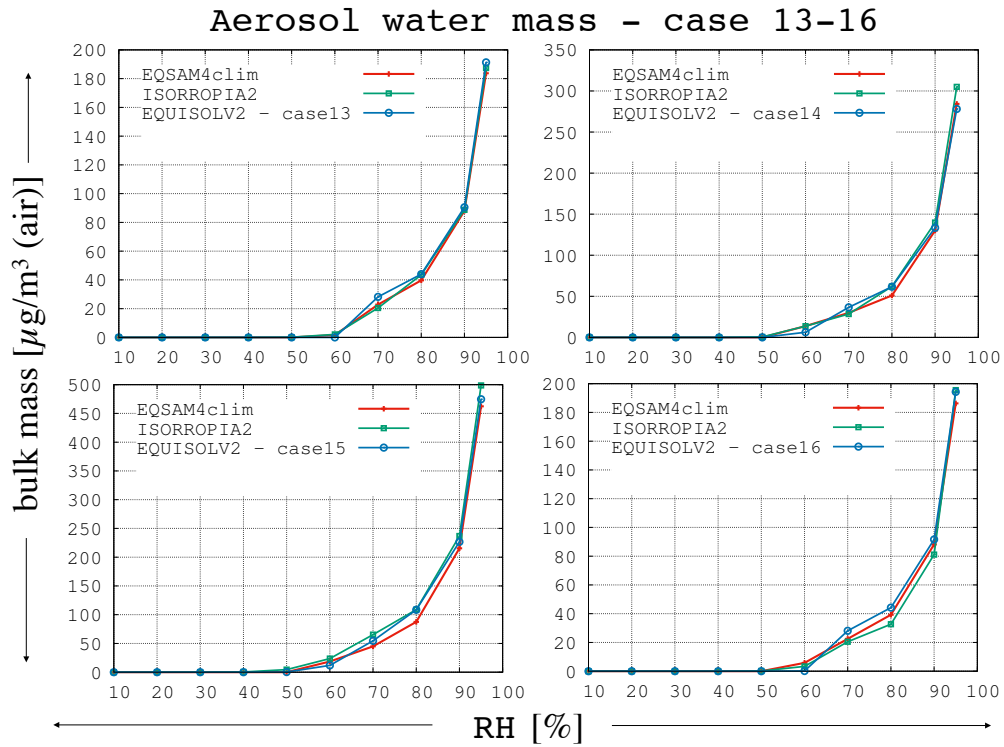


Figure S5.4: Case 13-16 of Figure S5 (Supplement).

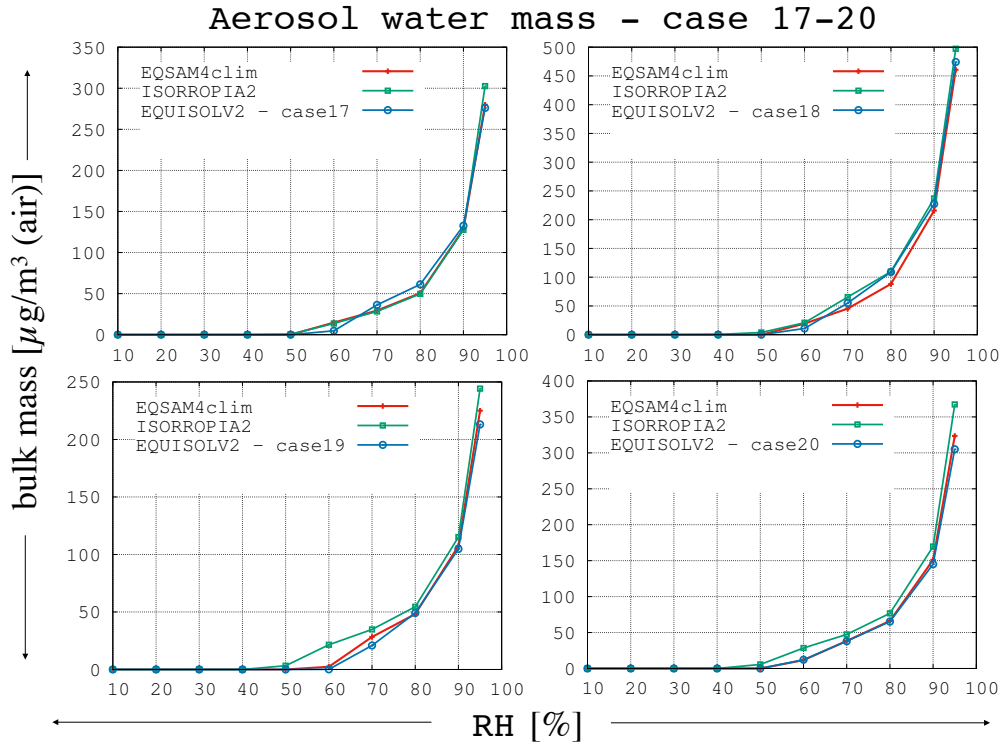


Figure S5.5: Case 17-20 of Figure S5 (Supplement).

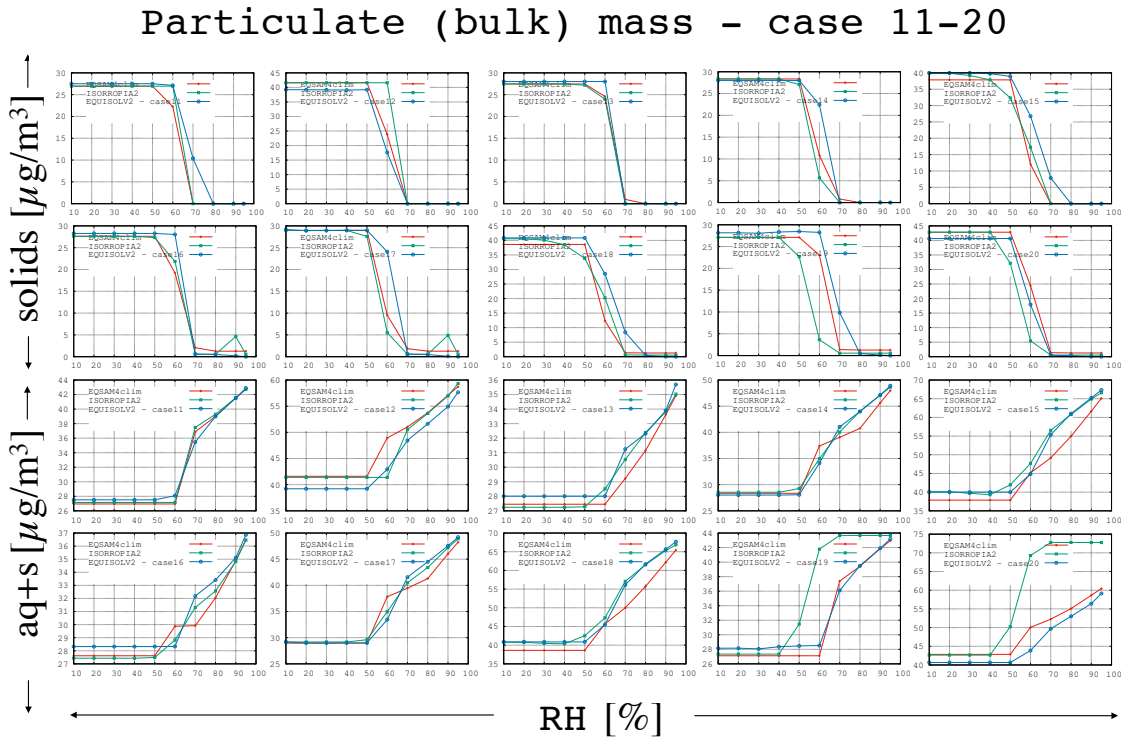


Figure S6: Extension of Figure 7 (main text): Total solid PM and liquid+solid PM.



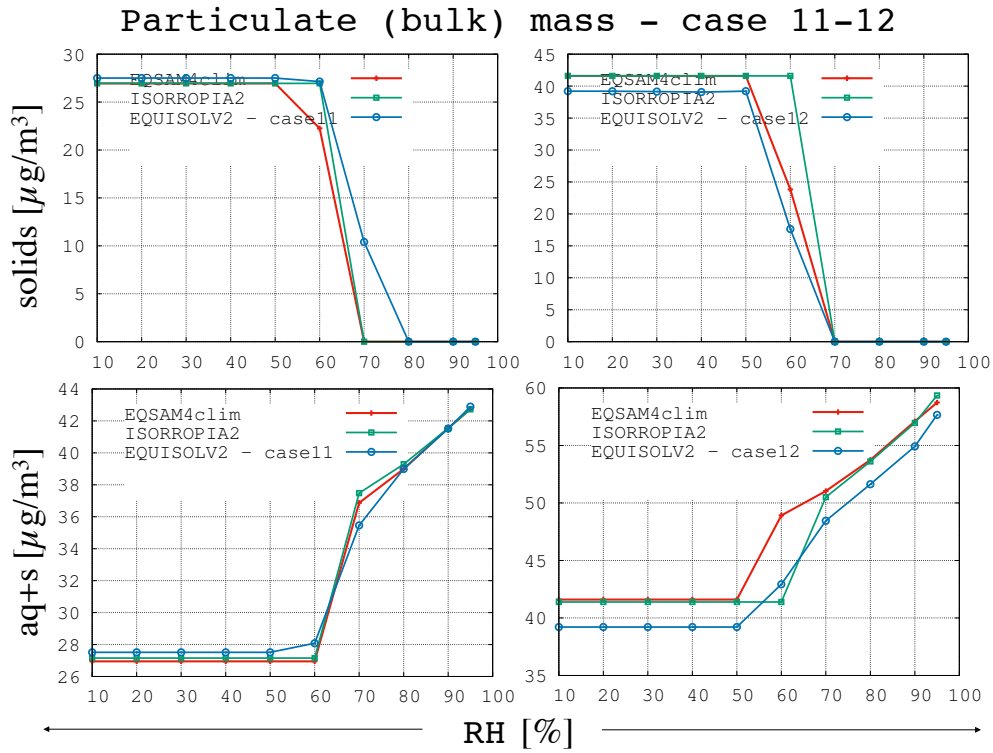


Figure S6.1: Case 11-12 of Figure S6 (Supplement).

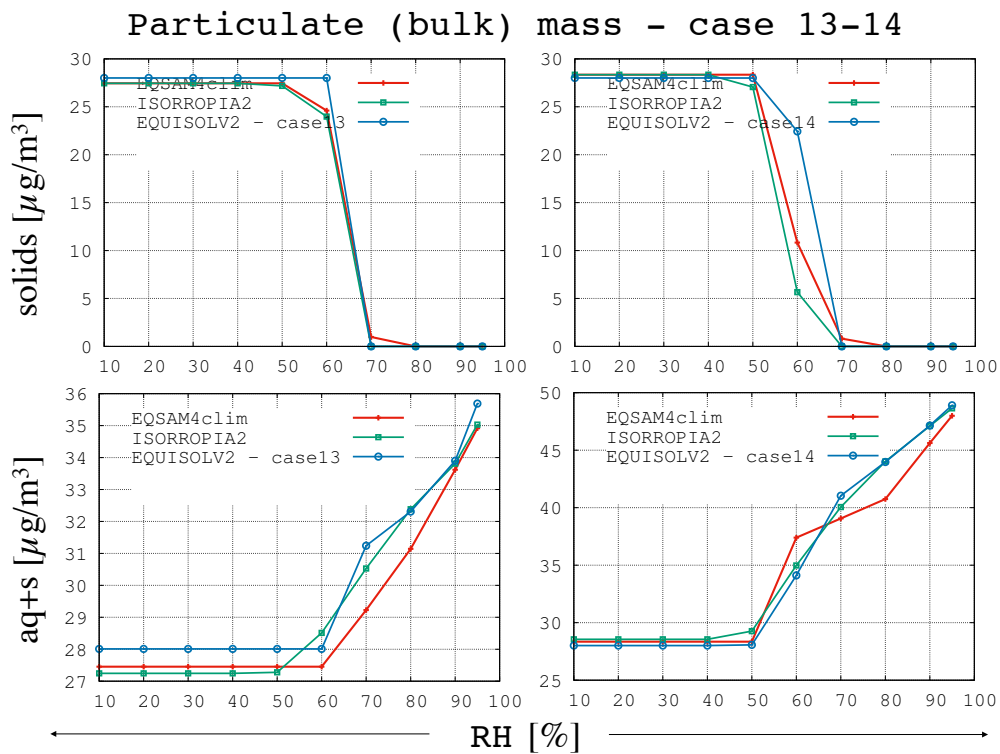


Figure S6.2: Case 13-14 of Figure S6 (Supplement).

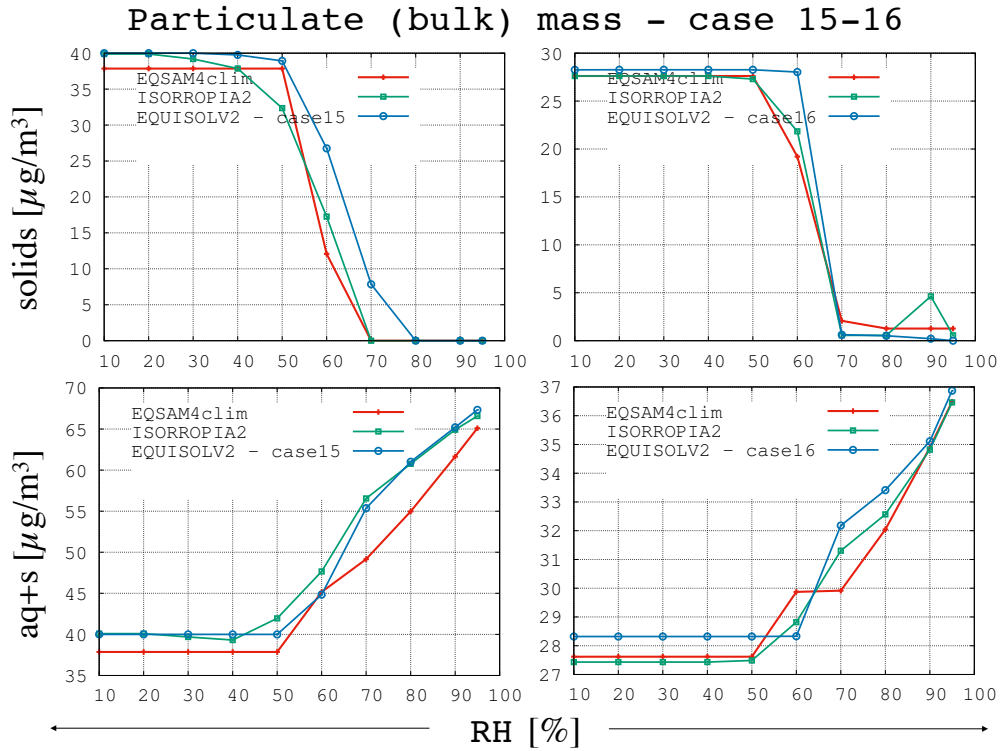


Figure S6.3: Case 15-16 of Figure S6 (Supplement).

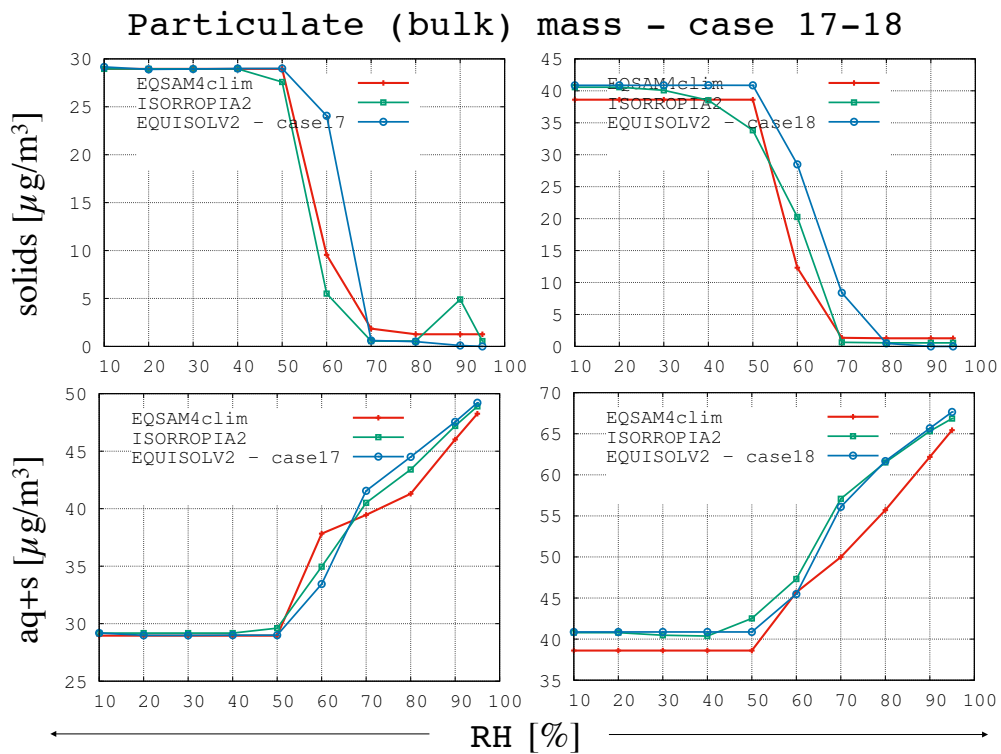


Figure S6.4: Case 17-18 of Figure S6 (Supplement).

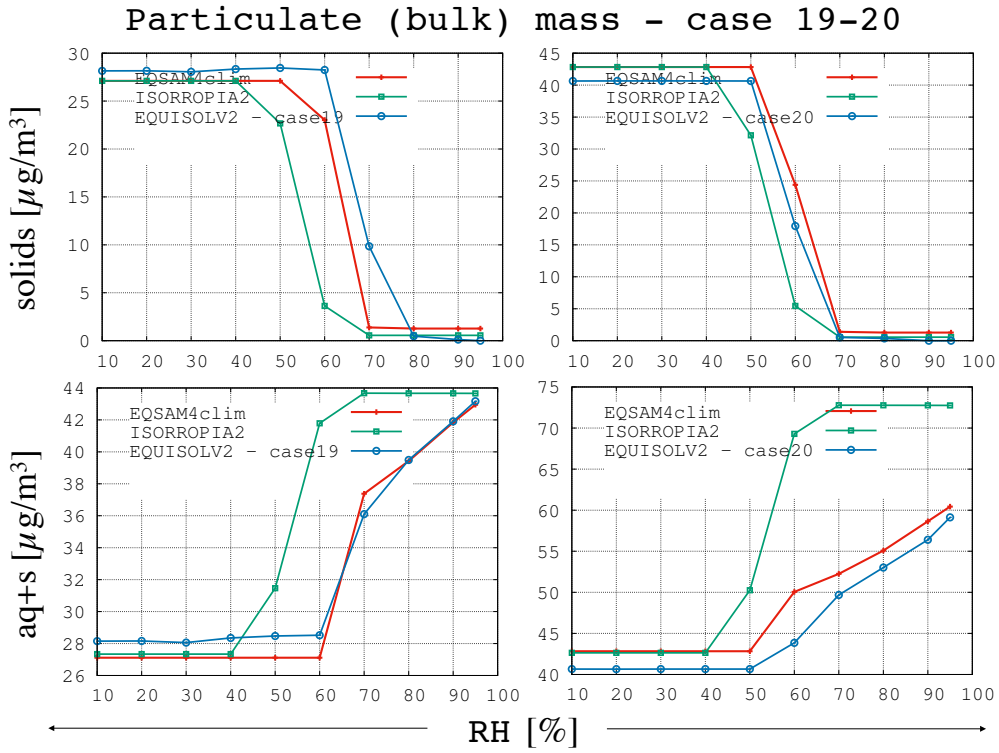


Figure S6.5: Case 19-20 of Figure S6 (Supplement).

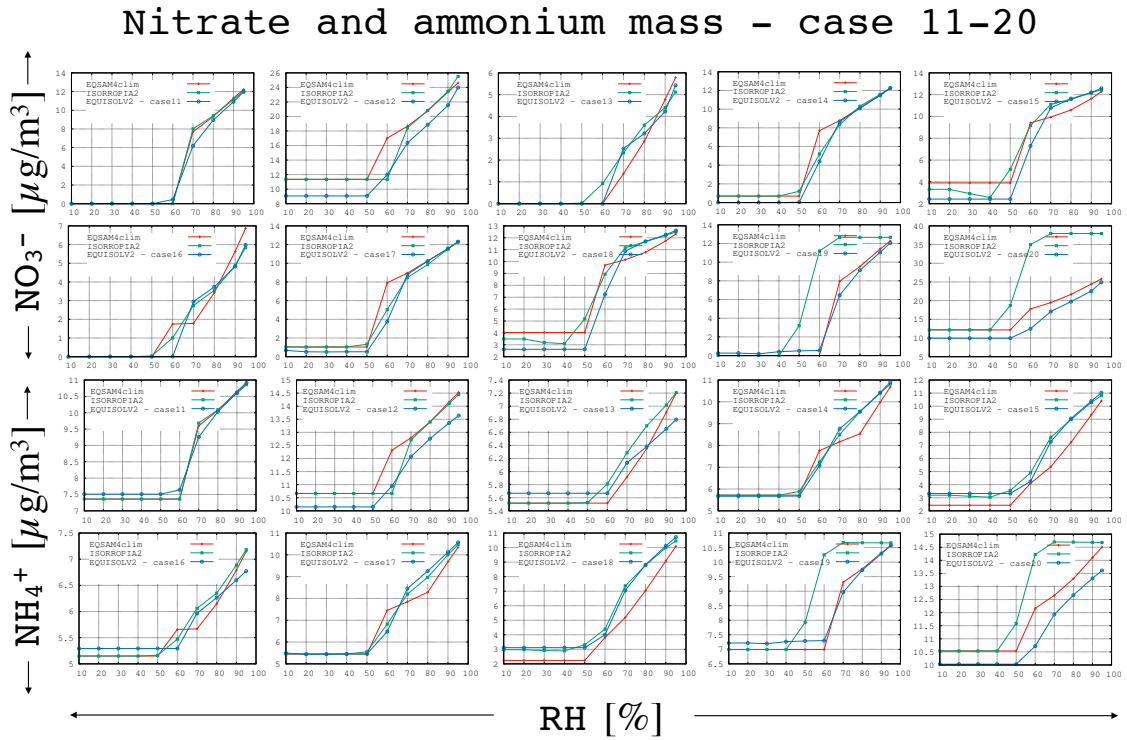


Figure S7: Extension of Figure 7 (main text): Bulk aerosol nitrate and ammonium.

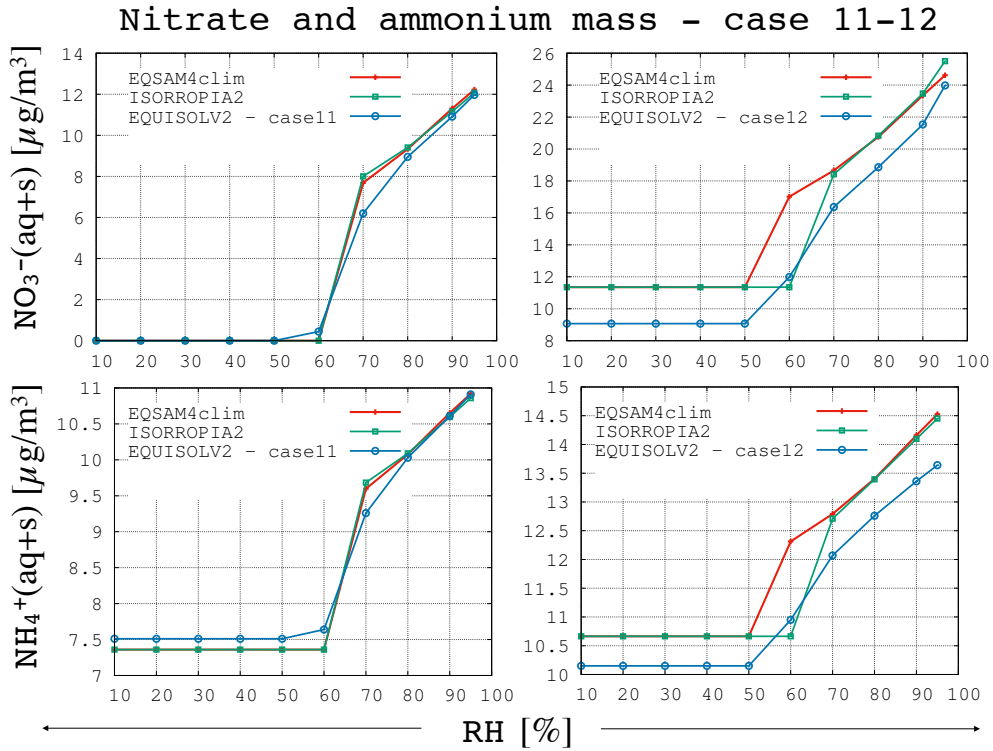


Figure S7.2: Case 11-12 of Figure S7 (Supplement).

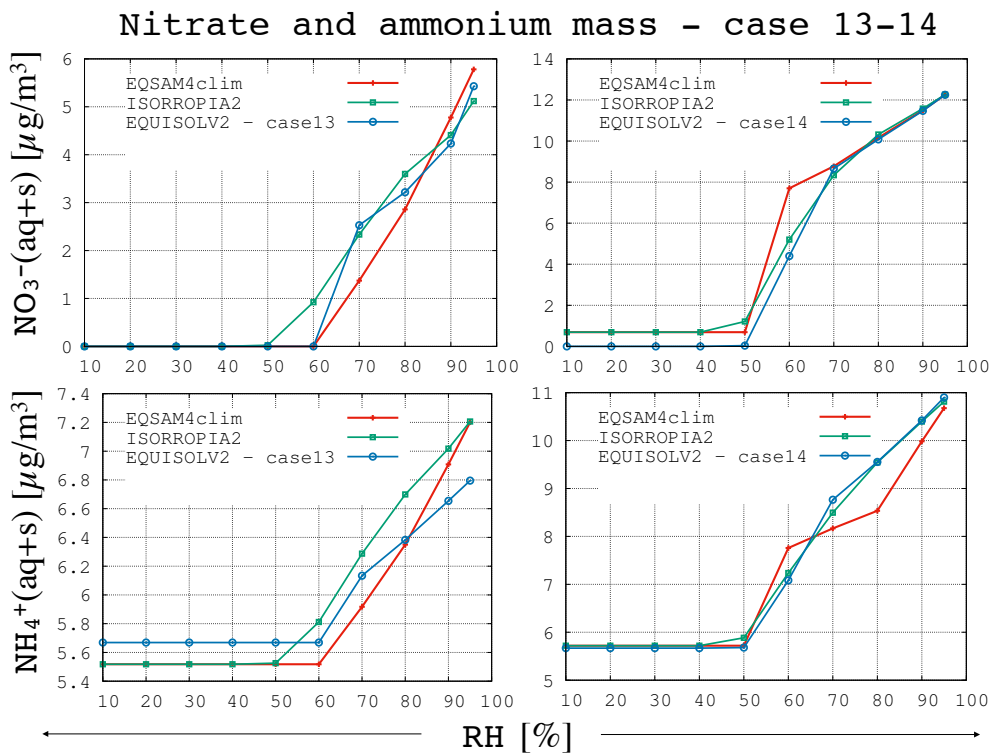


Figure S7.3: Case 13-14 of Figure S7 (Supplement).

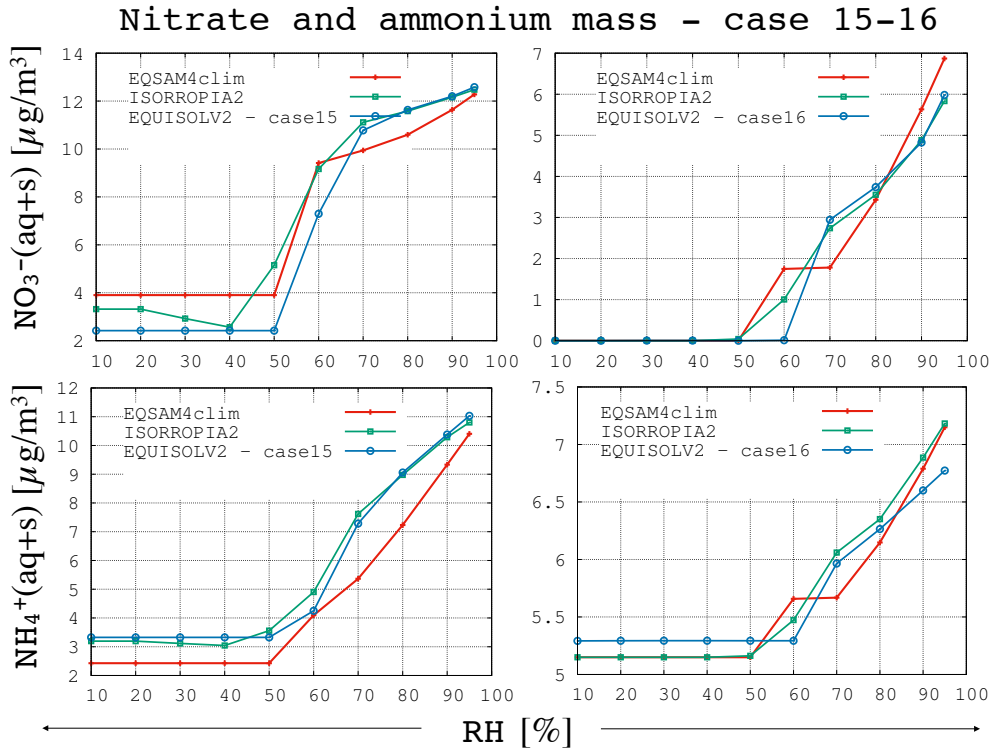


Figure S7.4: Case 15-16 of Figure S7 (Supplement).

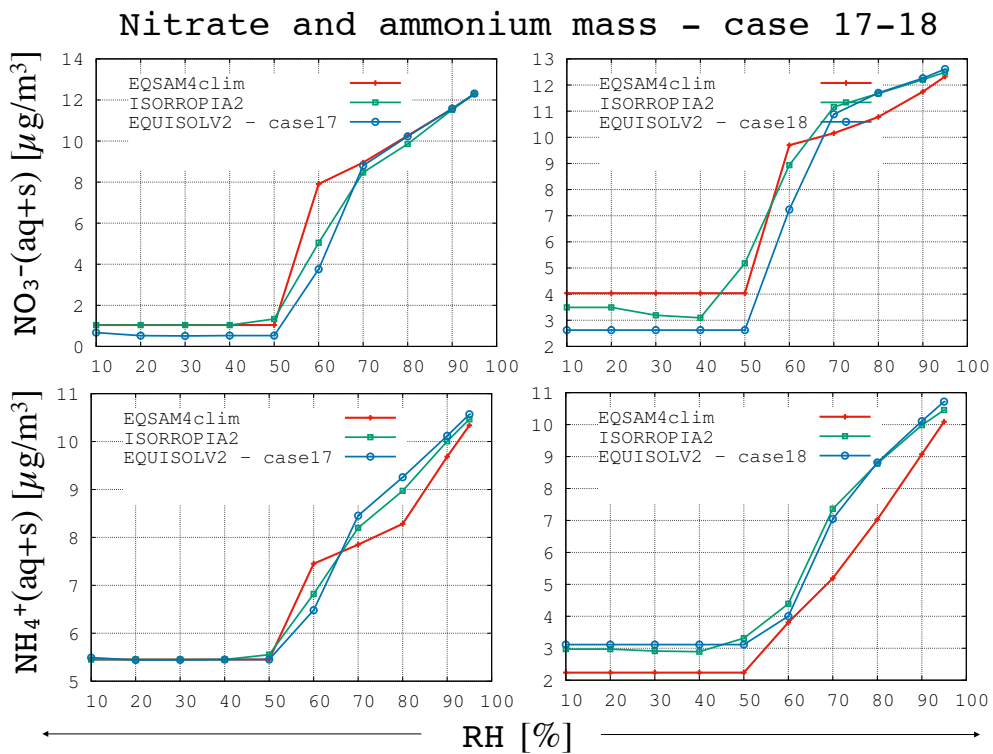


Figure S7.5: Case 17-18 of Figure S7 (Supplement).

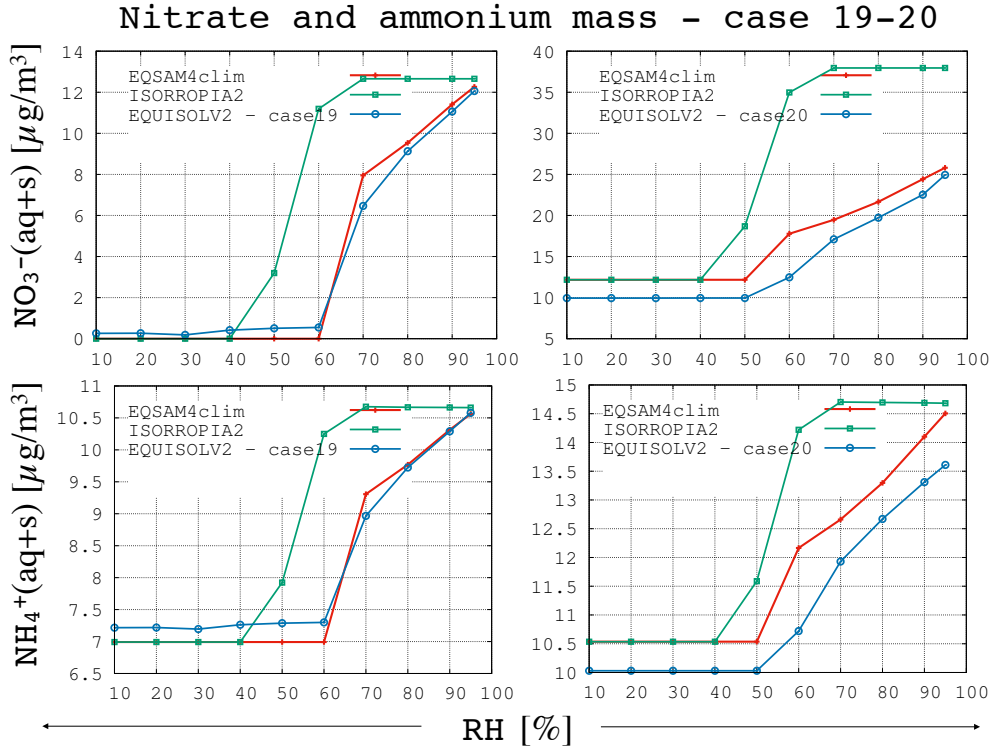


Figure S7.6: Case 19-20 of Figure S7 (Supplement).

### S3.4 Field observations – MINOS campaign

Extension of Figure 8 and 9 of Sec. 3.4. Figures S8 and Figure S9 show the gas-liquid-solid partitioning results of EQSAM4clim (red crosses) and ISORROPIA II (green squares). The equilibrium computations are based on lumped cation and anion concentrations, which were observed during MINOS in the aerosol fine and coarse mode, respectively. Fig. S8, panels (1-20), show the model results for the aerosol fine mode (from left to right, top to bottom): total aerosol water mass [ $\mu\text{g}/\text{m}^3(\text{air})$ ], total particulate (aqueous+solid) matter (PM) [ $\mu\text{g}/\text{m}^3(\text{air})$ ], total solid PM [ $\mu\text{g}/\text{m}^3(\text{air})$ ], total (aqueous+solid) PM [ $\mu\text{mol}/\text{m}^3(\text{air})$ ], and in [ $\text{nmol}/\text{m}^3(\text{air})$ ] the (lumped) ion concentrations of: ammonium ( $\text{NH}_4^+$ ), sodium ( $\text{Na}^+$ ), potassium ( $\text{K}^+$ ), calcium ( $\text{Ca}^{2+}$ ), magnesium ( $\text{Mg}^{2+}$ ), sulfate ( $\text{SO}_4^{2-}$ ) – both as totals (aqueous+solid) and solids -, as well as total bi-sulfate ( $\text{HSO}_4^-$ ) and the residual gases, hydrochloric acid (HCl), nitric acid ( $\text{HNO}_3$ ) and ammonia ( $\text{NH}_3$ ).

Fig. S9, panels (1-20), show the model results for the aerosol coarse mode (from left to right, top to bottom): total aerosol water mass [ $\mu\text{g}/\text{m}^3(\text{air})$ ], total particulate (aqueous+solid) matter (PM) [ $\mu\text{g}/\text{m}^3(\text{air})$ ], total solid PM [ $\mu\text{g}/\text{m}^3(\text{air})$ ], total (aqueous+solid) PM [ $\mu\text{mol}/\text{m}^3(\text{air})$ ], and in [ $\text{nmol}/\text{m}^3(\text{air})$ ] the (lumped) ion concentrations of: ammonium ( $\text{NH}_4^+$ ), sodium ( $\text{Na}^+$ ), potassium ( $\text{K}^+$ ), calcium ( $\text{Ca}^{2+}$ ), magnesium ( $\text{Mg}^{2+}$ ), sulfate ( $\text{SO}_4^{2-}$ ), bi-sulfate ( $\text{HSO}_4^-$ ), nitrate ( $\text{NO}_3^-$ ), chloride ( $\text{Cl}^-$ ), – all both as totals (aqueous+solid) and solids, except ammonium and bi-sulfate, which are omitted because of their very low (negligible) concentrations. Figures S8 and S9 are enlarged below, by Fig. S8.1-S8.5 and Fig. S9.1-S9.5, respectively to show the details. Despite the different approaches in the mixed solution treatment of EQSAM4clim and ISORROPIA II, EQSAM4clim is relatively close to the results of ISORROPIA II, capturing many details of the solid precipitation of individual compounds for both, the fine and coarse mode.

**Gas-liquid-solid Partitioning (fine mode)**  
 $Mg^{2+}$ - $Ca^{2+}$ - $Na^+$ - $HCl/Cl^-$ - $NH_3/NH_4^+$ - $HNO_3/NO_3^-$ - $H_2SO_4/HSO_4^-/SO_4^{2-}$ - $H_2O$

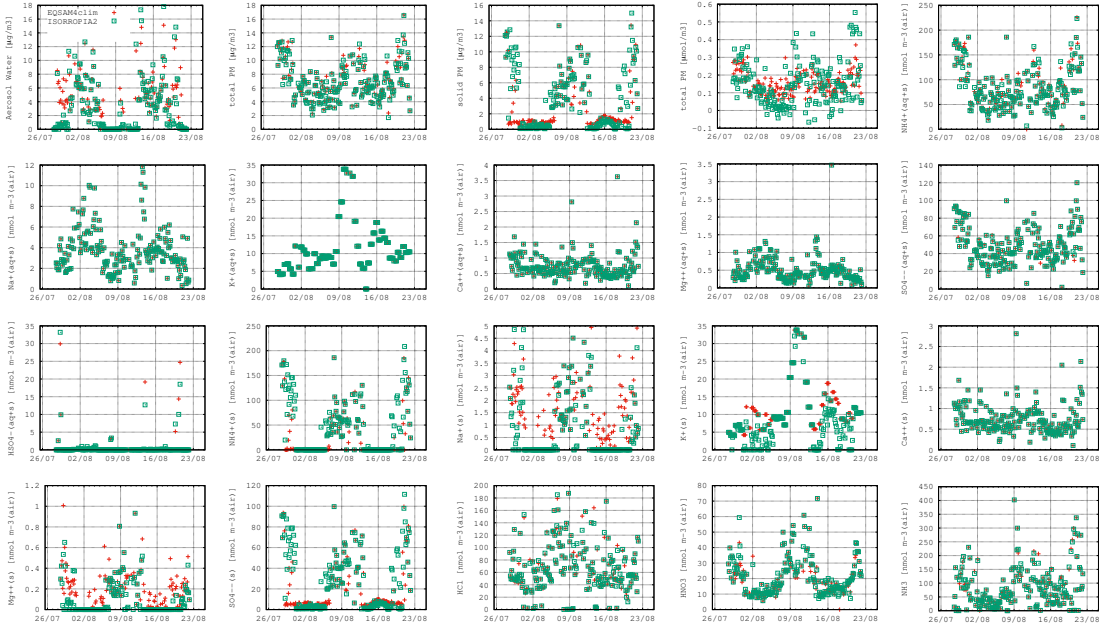


Figure S8: Extension of Figure 8 (main text): Aerosol water, total particulate matter and total solids [ $\mu g/m^3(air)$ ], the corresponding residual gases [ $\mu mol/m^3(air)$ ], and various ions for the fine mode. EQSAM4clim (red crosses), ISORROPIA II (green squares). A subset of four panels is shown in the following for better reading.

**Gas-liquid-solid Partitioning (coarse mode)**  
 $Mg^{2+}$ - $Ca^{2+}$ - $Na^+$ - $HCl/Cl^-$ - $NH_3/NH_4^+$ - $HNO_3/NO_3^-$ - $H_2SO_4/HSO_4^-/SO_4^{2-}$ - $H_2O$

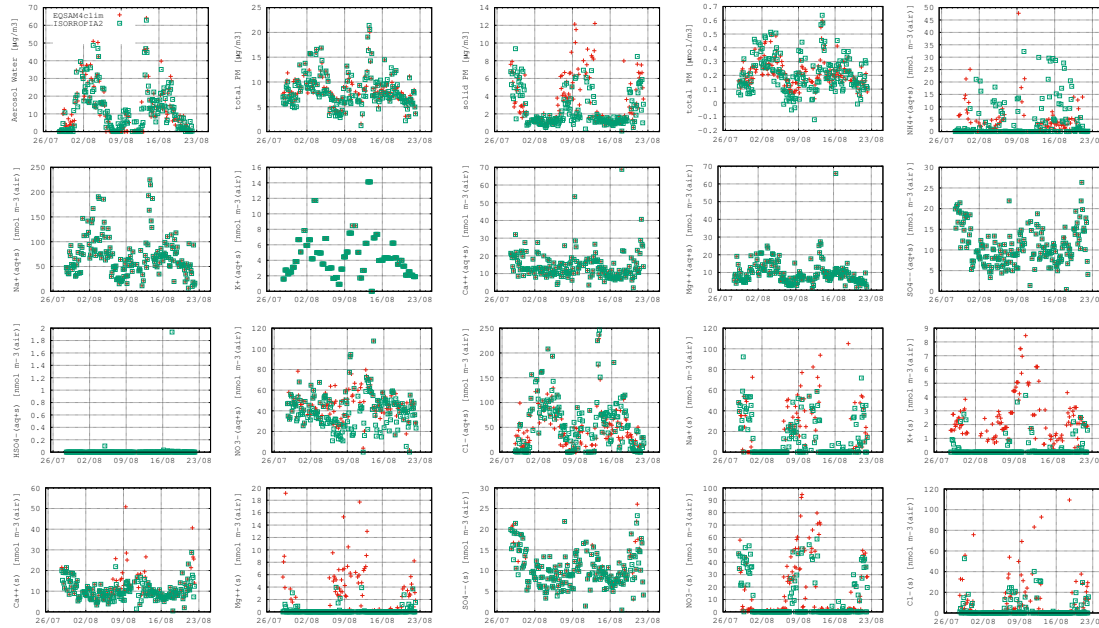


Figure S9: Extension of Figure S8 and Fig. 8 (main text) to the coarse mode.



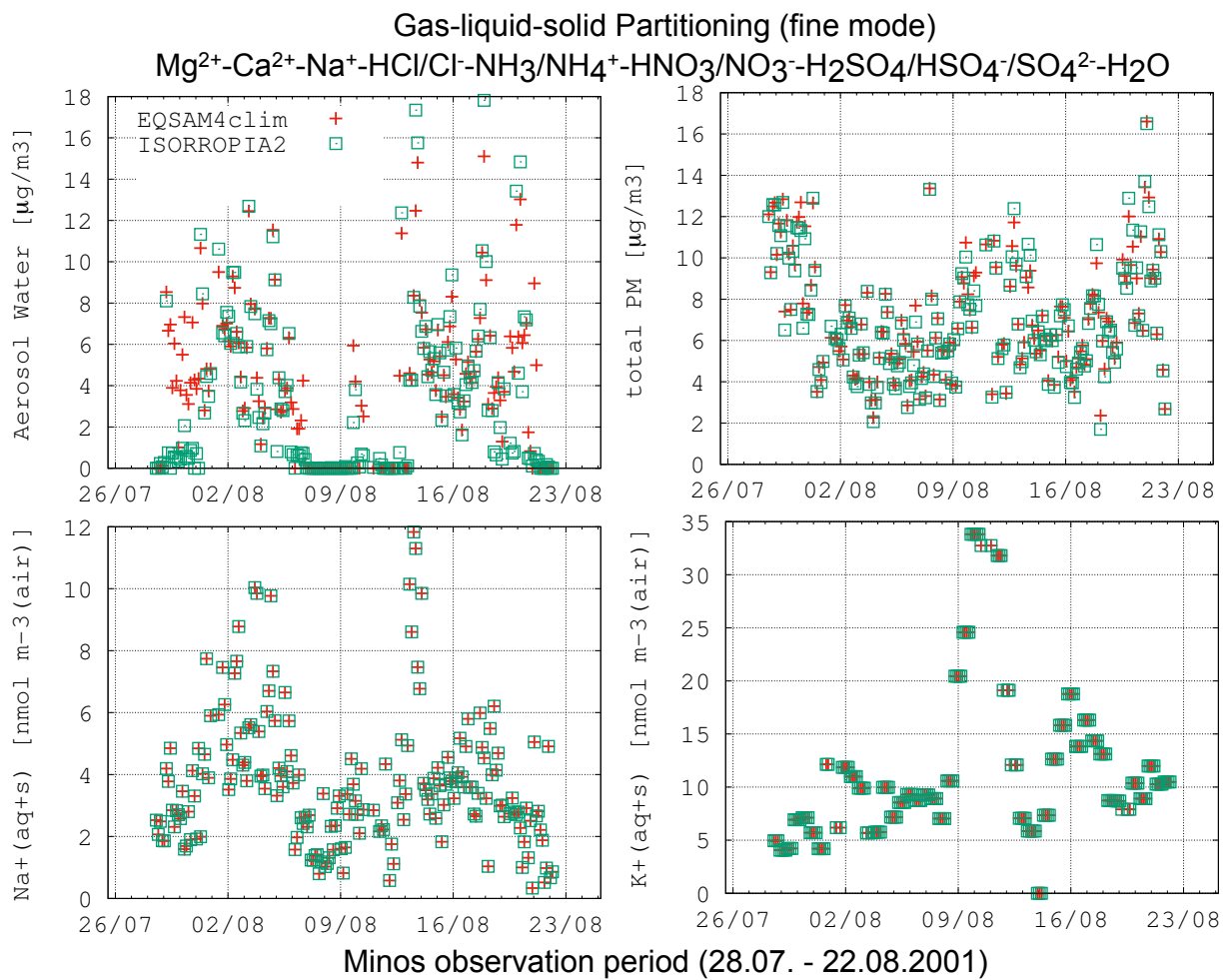


Figure S8.1: Details of Figure S8 (Supplement): Aerosol water(aq), total mass (aq+s), lumped  $Na^+$ (aq+s) and  $K^+$ (aq+s) (nano moles).



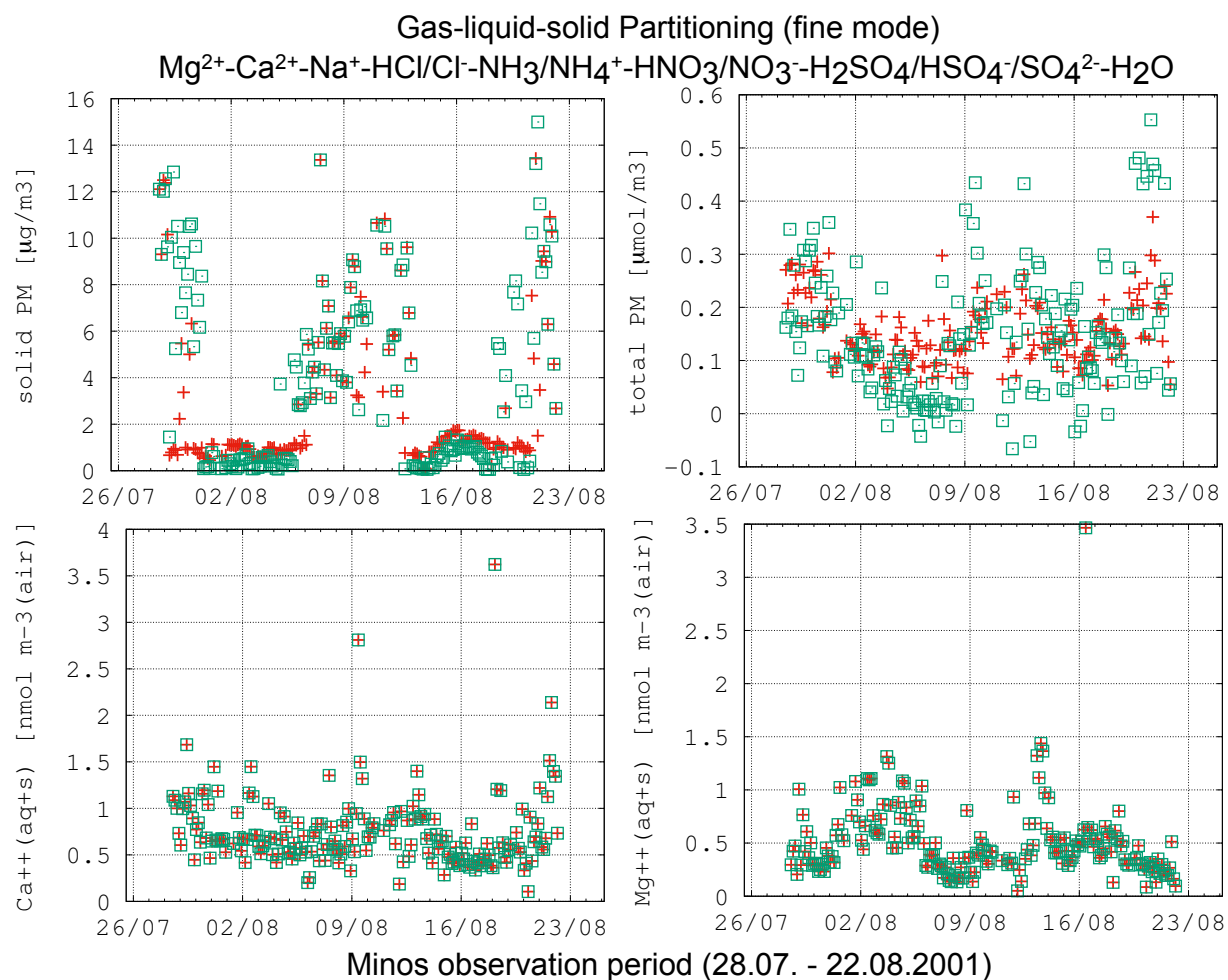


Figure S8.2: Details of Figure S8 (Supplement): solid mass(aq+s), total moles(aq+s), lumped  $Ca^{2+}$ (aq+s) and  $Mg^{2+}$ (aq+s) (nano moles).

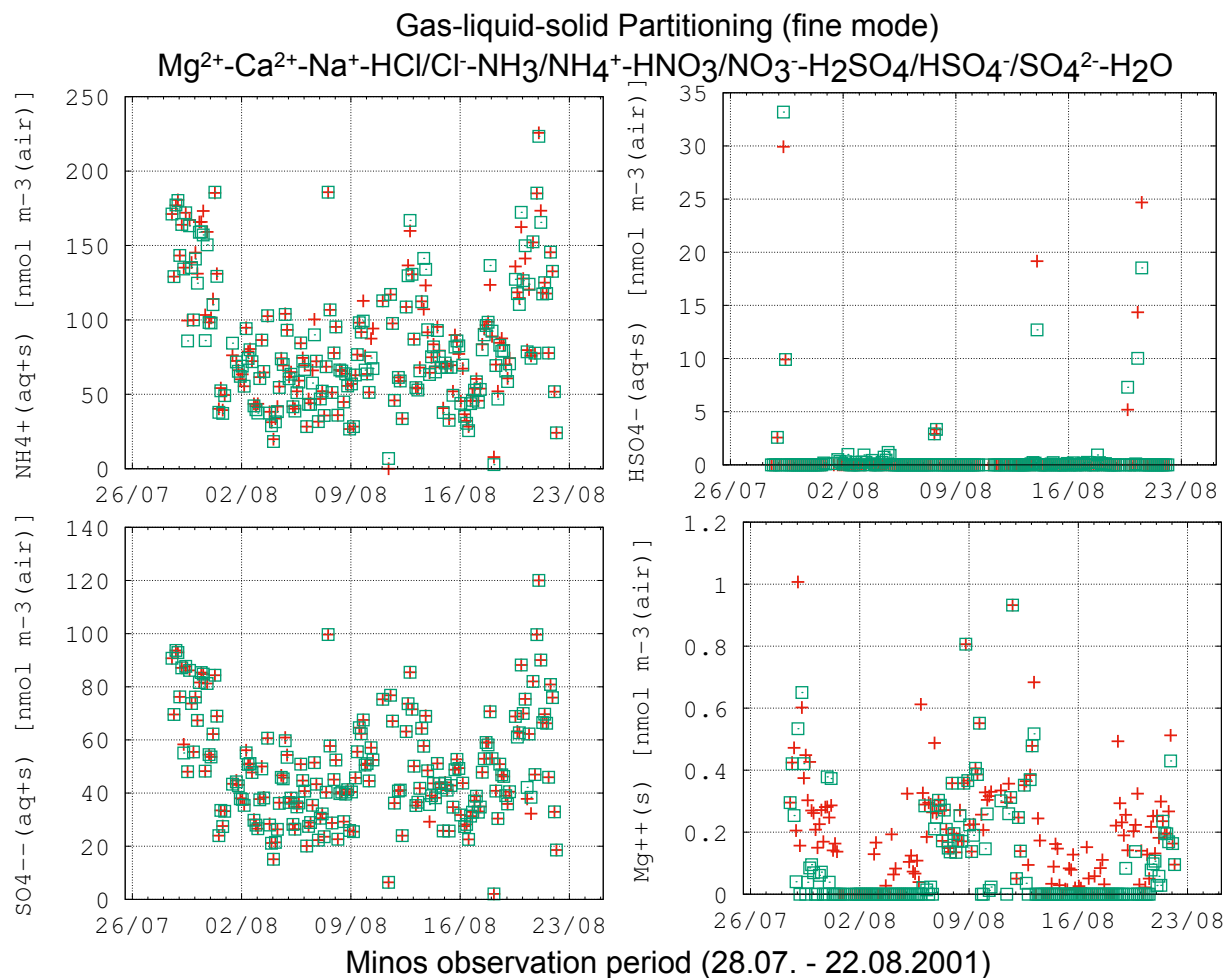


Figure S8.3: Details of Figure S8 (Supplement): Lumped  $NH_4^+$ (aq+s),  $HSO_4^-$ (aq+s),  $SO_4^{2-}$ (aq+s) and  $Mg^{2+}$ (s) (nano moles).

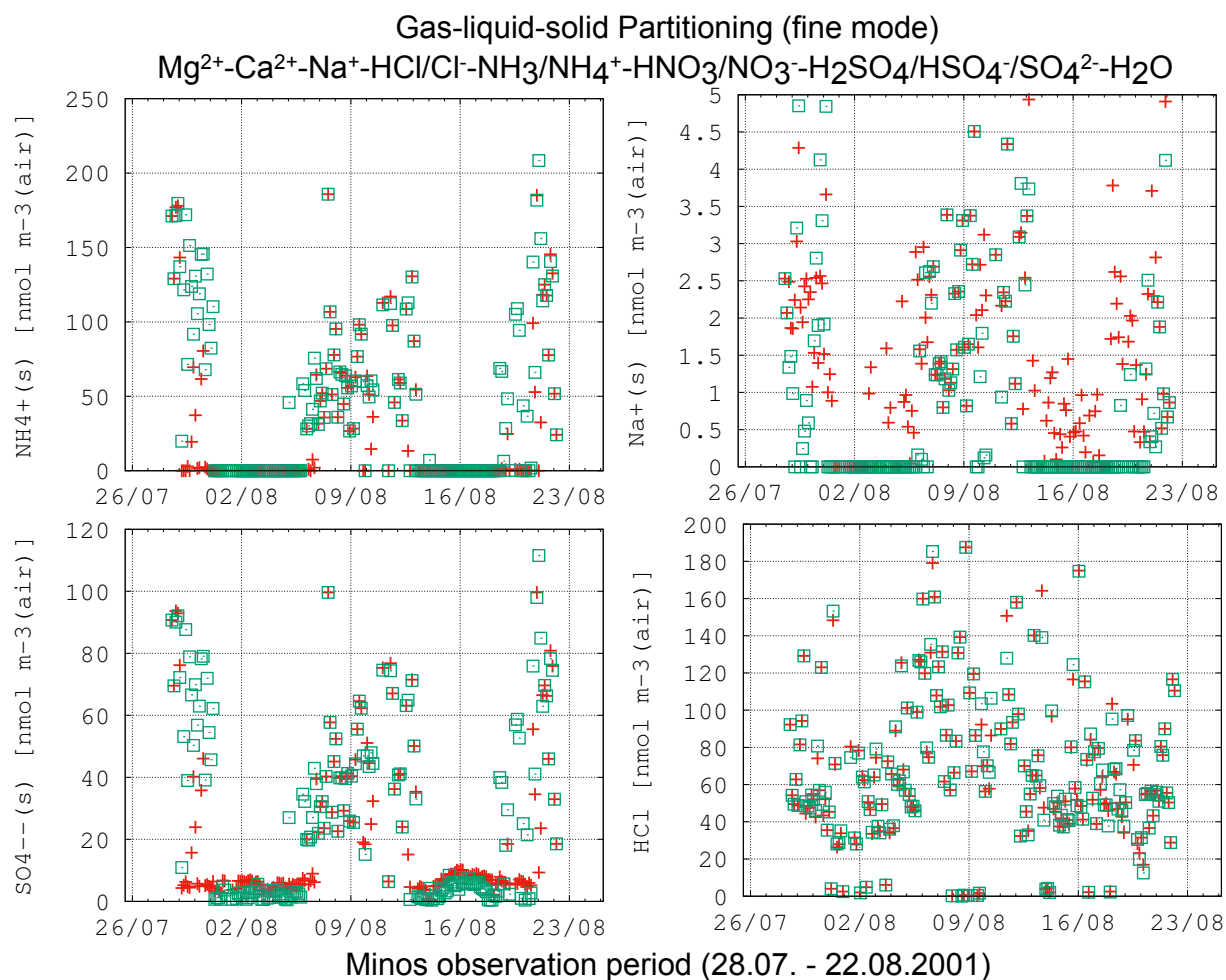


Figure S8.4: Details of Figure S8 (Supplement): Lumped  $NH_4^+(s)$ ,  $Na^+(s)$ ,  $SO_4^{2-}(s)$  and  $HCl(g)$  (nano moles).

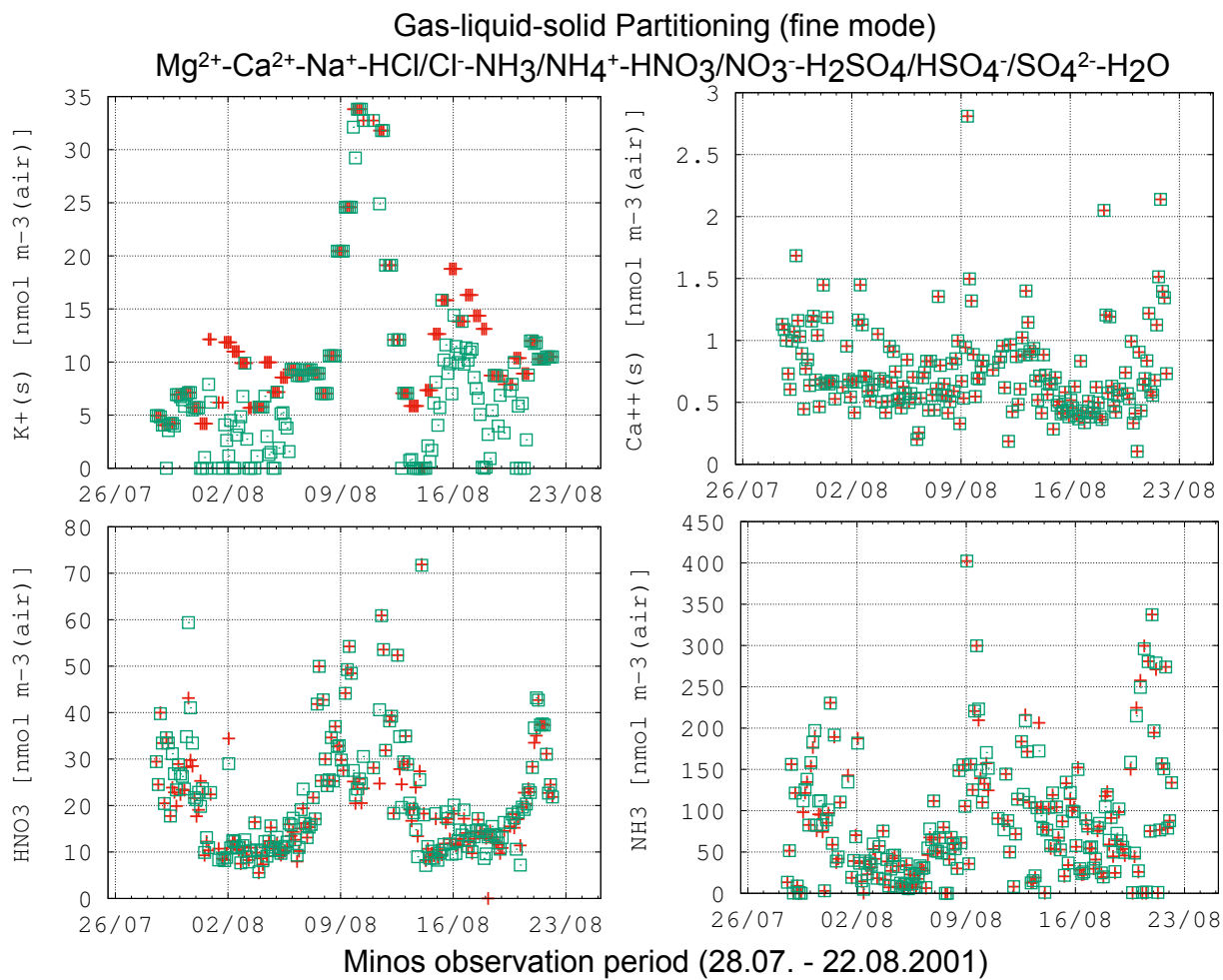


Figure S8.5: Details of Figure S8 (Supplement): Lumped  $K^+(s)$ ,  $Ca^{2+}(s)$ ,  $HNO_3(g)$  and  $NH_3(g)$  (nano moles).

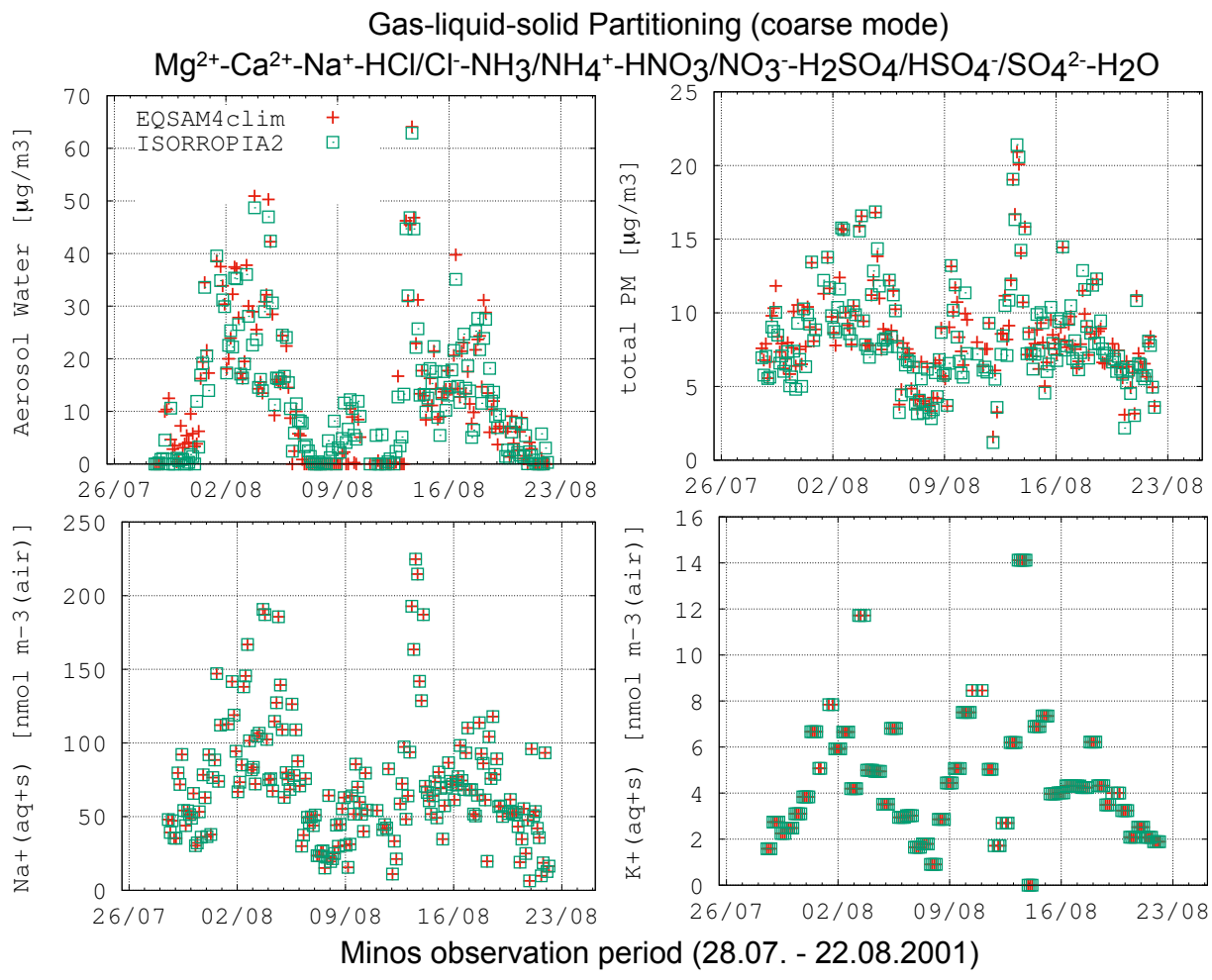


Figure S9.1: Details of Figure S9 (Supplement): Aerosol water(aq), total mass (aq+s), lumped  $Na^+$ (aq+s) and  $K^+$ (aq+s) (nano moles).

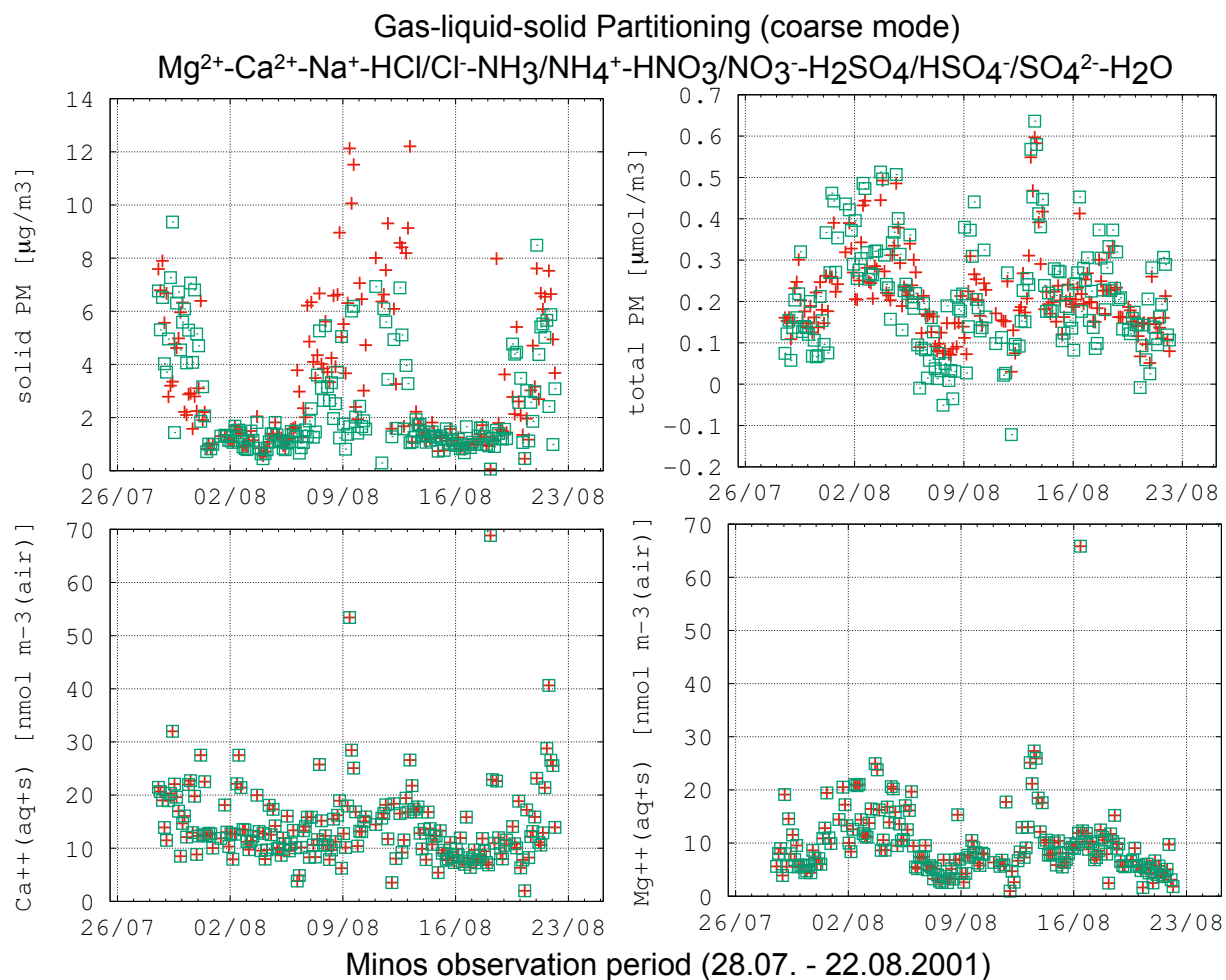


Figure S9.2: Details of Figure S9 (Supplement): solid mass(aq+s), total moles(aq+s), lumped  $Ca^{2+}$ (aq+s) and  $Mg^{2+}$ (aq+s) (nano moles).

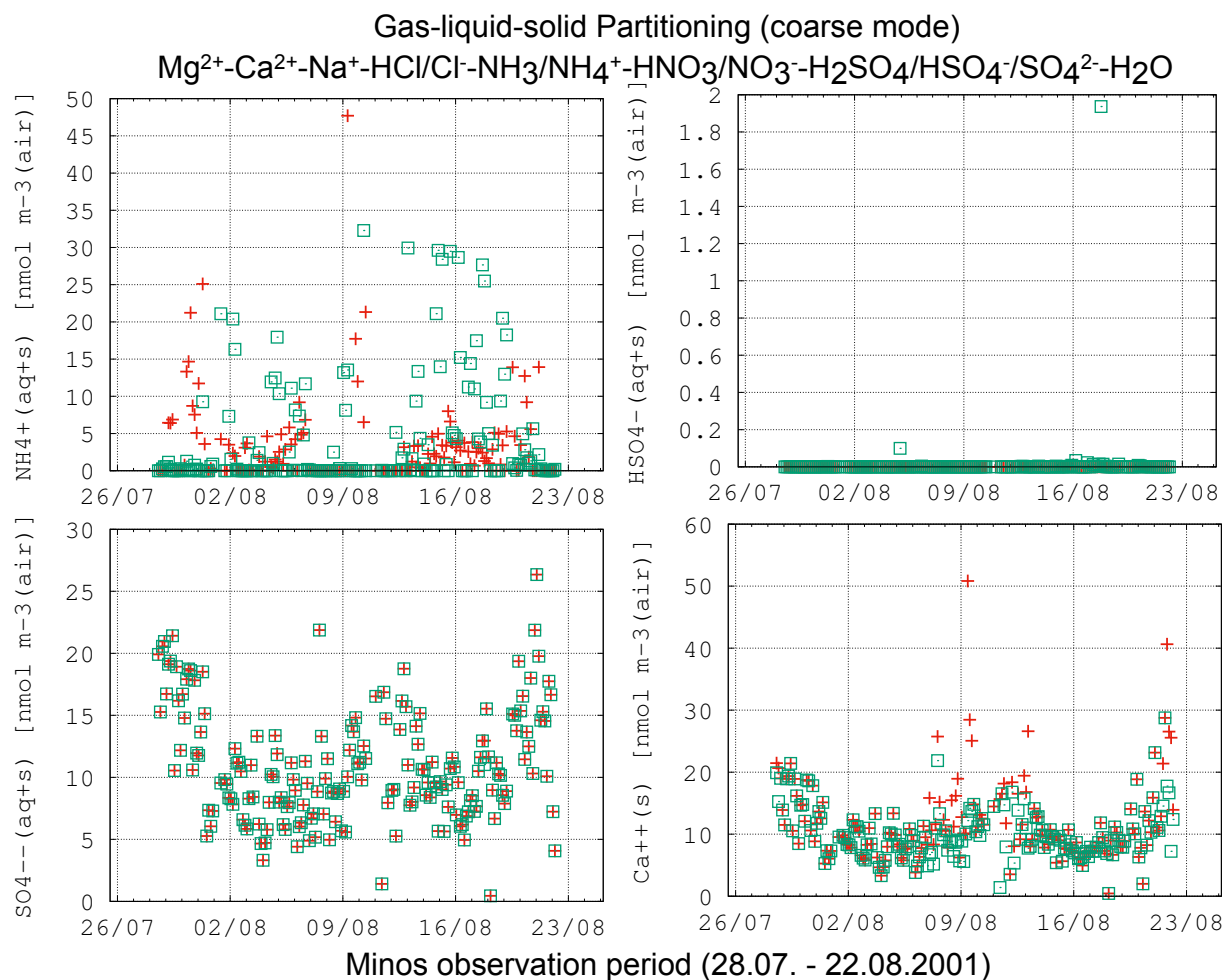


Figure S9.3: Details of Figure S9 (Supplement): Lumped  $NH_4^+$ (aq+s),  $HSO_4^-$ (aq+s),  $SO_4^{2-}$ (aq+s) and  $Ca^{2+}$ (s) (nano moles).

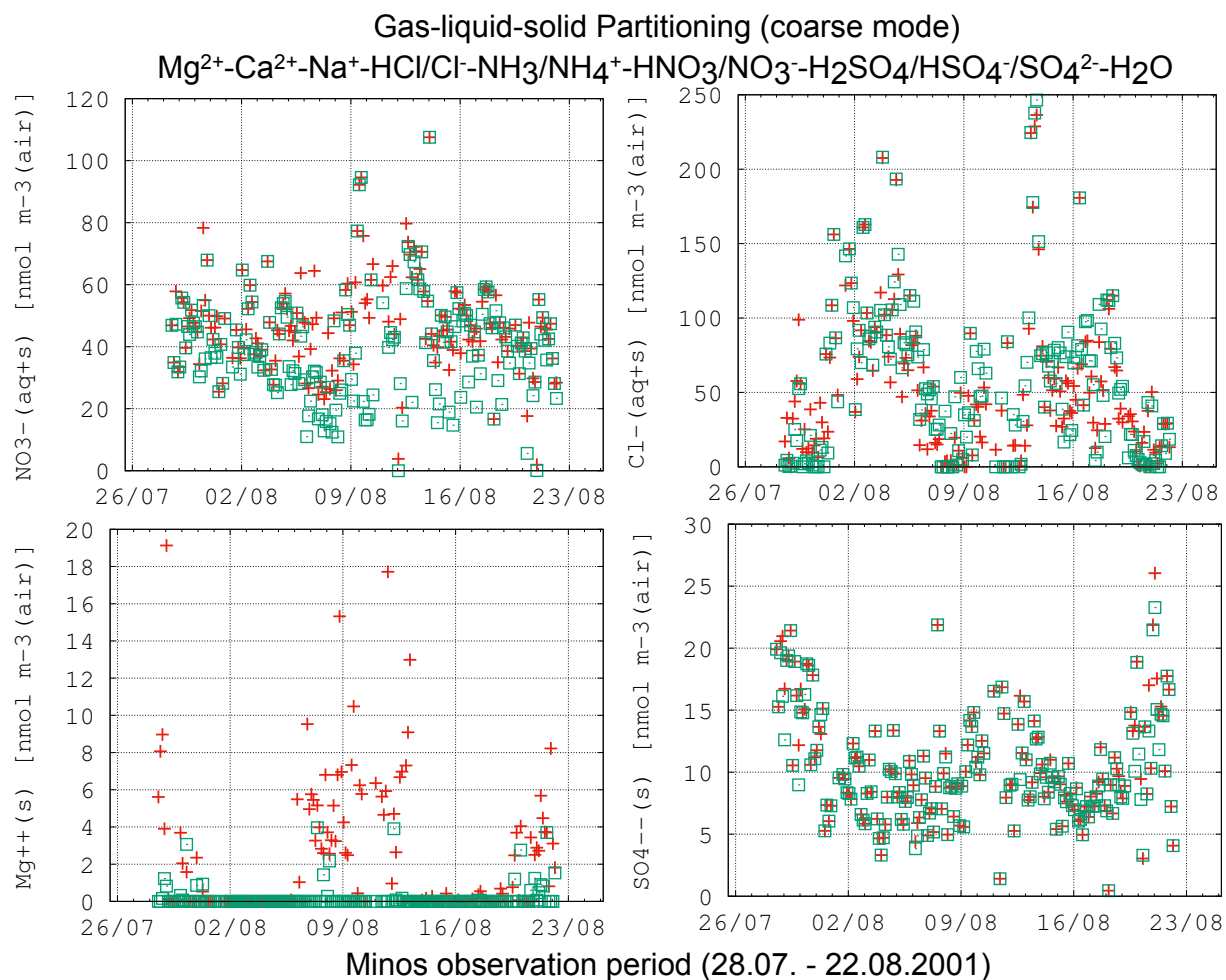


Figure S9.4: Details of Figure S9 (Supplement): Lumped  $NO_3^-(aq+s)$ ,  $Cl^-(aq+s)$ ,  $Mg^{2+}(s)$  and  $SO_4^{2-}(s)$  (nano moles).



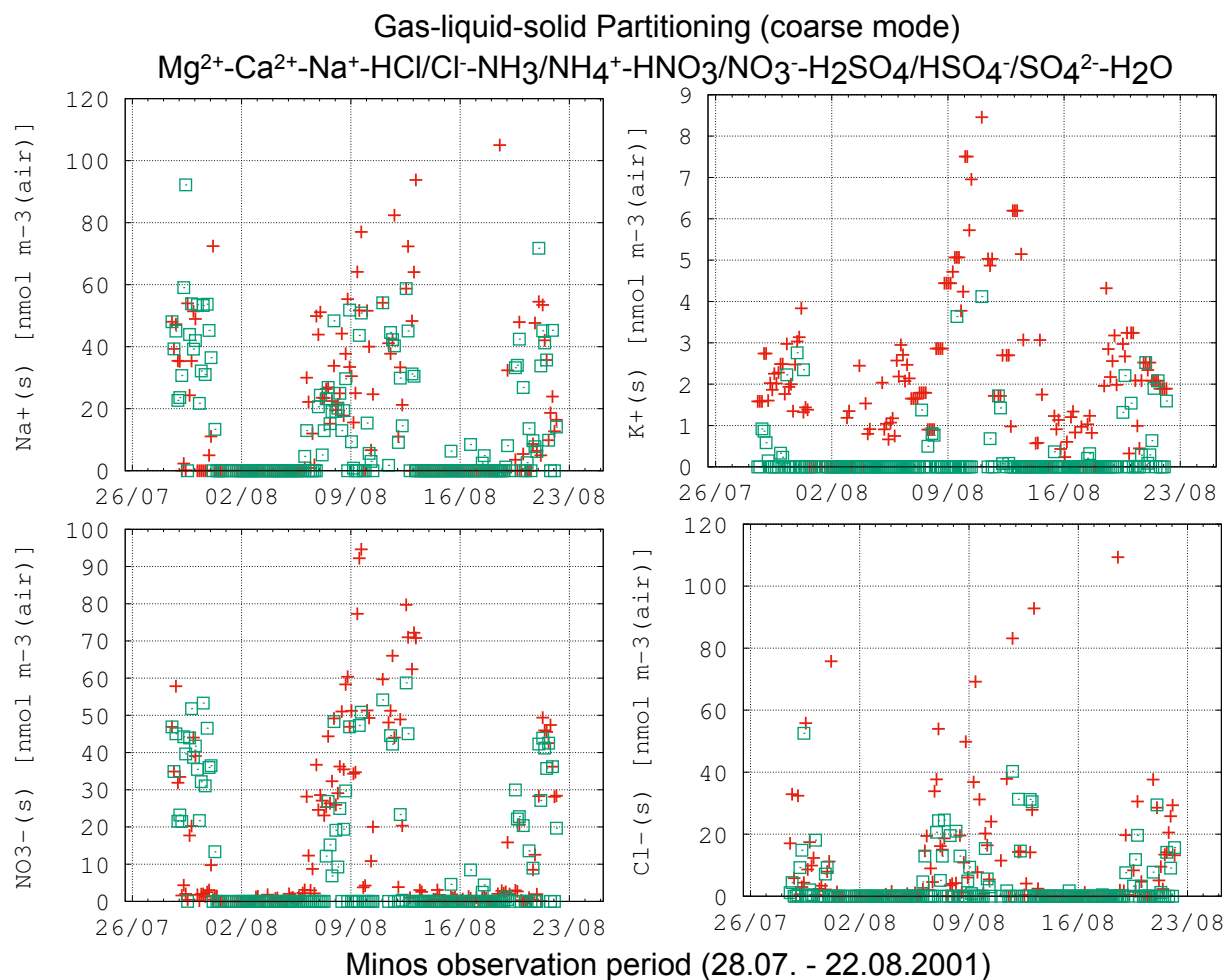


Figure S9.5: Details of Figure S9 (Supplement): Lumped  $Na^+(s)$ ,  $K^+(s)$ ,  $NO_3^-(s)$  and  $Cl^-(s)$  (nano moles).